

UNIVERSIDADE DE LISBOA
FACULDADE DE CIÊNCIAS
DEPARTAMENTO DE BIOLOGIA VEGETAL



**Single domain antibodies association to Lipid-guide drug
delivery as an innovative therapeutic strategy against cancer
stem cells**

Ana Carolina Malho Sousa

Mestrado Biologia Molecular e Genética

Dissertação orientada por:
Doutora Mafalda Castroi Ascensão Marques Videira
Doutora Maria Margarida Blasques Telhada

2017

Aos meus pais, por todo o esforço emocional e financeiro que fizeram

Para que eu tenha tido a oportunidade de fazer isto

À minha irmã que um dia será uma excelente dona de casa

Agradecimentos

Fazer agradecimentos seja para que fim for nunca é fácil e, ainda para mais, se eles forem escritos. Por muito bonitas que as palavras escritas sejam nunca serão suficientes para expressar o meu agradecimento.

Em primeiro lugar queria agradecer à professora Mafalda, por ter sido a única a dizer sim quando todos os outros diziam que não e me ter dado a oportunidade de pôr à prova a minha capacidade de raciocínio. Acho que o resultado está à vista. Ao Gonçalo e à Cláudia sem estas duas pessoas esta tese não tinha sido feita, e acabada, no tempo em que foi – “*No words can express my appreciation for you guys*” – Achei que deviam saber isso. E ao professor Luís, que apesar de não ser uma presença constante nas reuniões semanais era sempre uma alegria quando aparecia. Via-se claramente que era meu conterrâneo.

Um especial agradecimento ao meu babe Filipe Olim, que mesmo com um oceano a nos separar e uns horários loucos, conseguíamos sempre arranjar tempo para deprimir sobre a vida e rir das nossas asneiras. Foi assim que muita estupidez cometida nesta tese foi descoberta. À Diana que mesmo contra à minha vontade conseguia sempre tirar-me do laboratório, o que acabava sempre por ser bom.

À Débora Reis que mesmo não nos falando regularmente parece sempre que nunca nos separámos, e era sempre bom saber que havia sempre alguém na mesma situação que nós.

À Bárbara Correia, a minha parceira na “depressão” ao longo deste ano. Muitas foram as conversas, à hora de almoço, que tivemos sobre o quão deprimentes estavam as nossas vidas e quão loucas erámos por estarmos nesta situação. O nosso último ano bem que dava uma tese só por si só, já que as nossas células quase que parecem um espelho uma da outra. Quando uma sofria, a outra mais tarde ou mais cedo seguia o mesmo caminho. E foi um prazer ajudá-la quando me pediu.

Aos meus dois amigos de Moçambique dedico um parágrafo só para os dois, por isso não quero discussões. Vou começar pelo Clemente, só pelo simples facto da Arsénia me ter dado um parágrafo *super* pequeno. Ainda bem que tu percebias desta burocracia toda, porque deus me livre se passado este tempo todo se já cheguei lá. E também porque alguém tinha que me incentivar a fazer exercício. Lamento se não funcionou lá muito bem. Mas é sempre bom saber que alguém se preocupa connosco. Também é uma boa companhia para sair. Não gosta é que cheguem atrasadas. O mesmo já não se pode dizer da Arsénia. Durante este último ano em todas as saídas combinadas só uma única vez é que chegou a horas. De todas as outras chegava sempre depois da hora combinada. E, apesar de achar que eu sou um estoíro para o orçamento dela, era só para o dela que funcionava já que o meu ficava sempre bem no fim de um dia de compras. Mas não deixa de ser uma boa companhia para deprimir e ir às compras. Apesar de às vezes ela deprimir de uma forma estranha. Chegavam a existir vezes em que ficava na dúvida sobre quem estava a deprimir quem, e se ela estava a deprimir ou simplesmente os seus neurónios já não estavam a funcionar corretamente. Mas foi um enorme prazer tê-los conhecido e a Arsénia ter sido das primeiras pessoas com que falei neste mestrado. Por isso obrigada.

E, claro, como é obvio não podia deixar de agradecer ao João Coelho. Aqui está uma pessoa que sabe sempre dizer a palavra certa no momento certo, mesmo quando ele acha que não, ou se sente mal por não saber o que dizer. Quando toda a gente fugia com medo que eu pudesse extravasar a minha raiva para cima delas, ele mesmo “tendo medo” (que eu sei que é a brincar) nunca fugiu e ainda me incentivava a libertá-la, mas tinha sempre um abraço para dar e às vezes isso é o que importante. Só o facto de estar lá, presente e disposto a ouvir é o que mais importa, mesmo que nunca o tenha dito. Mas espero que ele saiba.

Abstract

Mesenchymal-like adenocarcinomas are a subtype of triple-negative breast cancer (TNBC) adenocarcinomas that, as any TNBC, lack predictive biomarkers, such as estrogen receptor (ER), progesterone receptor (PR) and prognostic biomarkers, such as HER2. Thus, it presents a poor prognosis and aggressive clinical behavior. Since they can exhibit a stem-like phenotype, they are generally called cancer stem cells (CSCs) and overexpress some surface markers, such as CD44.

CD44 is a transmembrane glycoprotein that has been linked to diverse intracellular mechanisms, from being a co-receptor for growth factors and cytokines uptake to sustain cell' survival, proliferation and invasion. Besides overexpressing CD44, MDA-MB-231 breast cancer cells also express high levels of mesenchymal proteins, such as vimentin. Vimentin is responsible, among other things, for cell invasion and motility, and considered one marker of epithelial-to mesenchymal transition (EMT). Because they overexpress P-glycoprotein (P-gp), a membrane drug efflux pump, the cytotoxic drug is not accumulated in the cytoplasm but recycled to the outside of cells.

Hence the necessity to develop new therapies that, besides targeting this subpopulation, can overcome the activity of P-gp. In the last few decades, nanomedicines are becoming the “holy grail” of cancer treatments because they are directly targeted to the cancer cells, based on the ERP (enhanced retention and permeabilization) effect, and by being functionalized against a specific surface marker deliver the cytotoxic drug to a specific type of cancer.

Bearing in mind that nanoparticles preferably enter the cell via endocytosis, the main goal was to assess which type of endocytosis pathway is used in the uptake of functionalized and non-functionalized plain micelles in MDA-MB-231 breast cancer cells. Moreover, the aim of this work also comprised the determination of whether salinomycin would affect expression of vimentin and if the type of polymer used to make the micelles would mask salinomycin from the action of P-gp.

Here we show that non-functionalized micelles are uptaken by a caveolae-mediated process and that uptake of functionalized micelles is done through a CD44-mediated endocytosis process. We also show that functionalization can delay the entry of these micelles by, at least, 30 minutes. Functionalized micelles not only recruit caveolin but also increase the expression of CD44 in the membrane surface, contributing to the idea that once CD44 receptor is activated, the cytoplasmic domain translocates to the nucleus and transcribes the CD44 gene.

P-gp intracellular localization changes according to the treatment applied. In non-treated cells, it is mainly localized in the endoplasmic reticulum and Golgi apparatus, while in the presence of micelles it is localized not only in those organelles, but also in endosomes, and its activity is constant after 30 minutes and 1 hour of incubation. When treated with free salinomycin, P-gp accumulation increases in the endoplasmic reticulum and plasma membrane as a response to drug accumulation. MDA-MB-231 breast cancer cells treated with free or loaded salinomycin show an increase in the expression of the mesenchymal protein vimentin.

Thus, salinomycin may not be the best anticancer agent to kill breast cancer stem cells, but the micelles used in this work have a great potential to become a good transporter to have an intracellular accumulation of any cytotoxic drug. Either for functionalized and non-functionalized micelles, caveolin protein is the intervening player in the internalization of these micelles. In the presence of functionalized micelles, there is an increase in CD44 expression.

Key words: Breast cancer; CD44; P-glycoprotein; nanoparticles; endocytosis

Resumo

O cancro da mama triplo negativo (TNBC) é o tipo de adenocarcinoma que mais interessa aos investigadores e patologistas, uma vez que não responde aos tratamentos cancerígenos mais comuns. Este caracteriza-se pela ausência dos marcadores preditivos, tais como recetores de progesterona (PR) e de estrogénio (ER), que elucidam sobre a resposta de um paciente a uma terapia, e dos marcadores de prognóstico, tais como HER2, cuja presença ou ausência indica o risco de recorrência e mortalidade.

Um dos subtipos que nos interessa, e é utilizado neste trabalho, designa-se por tipo mesenquimal. Este tipo de cancro é caracterizado por desenvolver mecanismos que contribuem para a transição epitelial-mesenquimal, tal como a via do PI3K/AKT e mTOR. Para se tornarem células mesenquimais, as junções aderentes e apertadas são destruídas e a E-caderina é degradada. A supressão da expressão de genes epiteliais leva à ativação de genes mesenquimais e à reorganização do citoesqueleto de forma a permitir a migração e invasão celular. Uma das proteínas resultantes desta ativação é a vimentina que, sendo um filamento intermédio, tem a sua função dependente de um ciclo de fosforilação e desfosforilação. Na última década muitos são os papéis associados a esta proteína, nomeadamente manter a integridade celular durante a endocitose e participar na via PI3K/AKT como efetor do PI3K.

Por apresentarem características muito semelhantes às células estaminais são geralmente designadas de células cancerígenas tipo estaminais (*cancer stem cells – CSCs*). Dada a sua capacidade de diferenciação e renovação conseguem reconstituir a heterogeneidade inicial do tumor. As CSCs diferem das restantes células cancerígenas porque estimulam a expressão de recetores membranares, tais como o CD44, e reprimem a expressão de outros, como o CD24. O marcador do fenótipo estaminal destas células mais utilizado é o recetor CD44 e, na nossa opinião, tem o potencial para se tornar um biomarcador no tratamento do cancro.

O CD44 é uma glicoproteína transmembranar codificada por 20 exões. A forma mais expressa, e a de menor peso molecular, é a forma *standard* (CD44s), na qual existe apenas os exões constantes (exões 1-5 e exões 16-18). A inserção dos exões variáveis (exões 5-15 e 19-20) cria isoformas de maior peso molecular e a sua expressão depende do tipo de tecido e do microambiente extracelular. O domínio extracelular deste recetor regula a interação com a matriz extracelular durante a migração celular. A proteólise deste recetor leva à formação de um fragmento solúvel, correspondente ao domínio extracelular, e a um fragmento de 12 kDa, correspondente ao domínio intracelular, que tem a capacidade de se deslocar para o núcleo e ativar a transcrição do próprio gene CD44 e do fator de transcrição Twist. Trata-se de um recetor cuja função tem sido associada a vias de sinalização intracelular, tais como a via PI3K/Akt e MAPK-Ras, que regulam a sobrevivência, proliferação e invasão celular.

Um dos obstáculos mais importantes que qualquer fármaco encontra no momento em que alcança uma célula cancerígena é o transportador transmembranar designado de P-glicoproteína (P-gp). Esta bomba de efluxo é ativamente sobre expressa em células cancerígenas e tem a capacidade de transportar fármacos e outro tipo de moléculas contra o seu gradiente de concentração, o que significa que o fármaco quando interage com o domínio transmembranar desta proteína é efluxado para o citoplasma, evitando a sua acumulação no citoplasma, conferindo a estas células um fenótipo de resistência a fármacos (*Multidrug Resistance - MDR*).

Os nanotransportadores são sistemas à escala nanométrica constituídos por pelo menos dois componentes, no qual um deles é o agente ativo (neste trabalho trata-se da salinomicina) e o outro que é responsável pela proteção do agente ativo e o seu transporte (que neste trabalho será o poloxamero). A principal via de entrada destas partículas na célula é através de um processo de endocitose. No caso de partículas de tamanho nanométrico, como as do presente trabalho, são internalizadas por um processo dependente de clatrina ou por um processo dependente de caveolae.

Endocitose dependente de clatrina é o mecanismo de endocitose mediada por recetor mais importante. Quando uma partícula funcionalizada se liga a um recetor membranal específico ocorre o

recrutamento de proteínas endocíticas, tais como AP2 e claterina, de modo a se formar uma vesícula (revestida por claterina) que contém as nanopartículas, que se separa da membrana através da ação da dinamina. Uma vez no citosol a claterina é degradada e as vesículas formadas deslocam-se ao longo do citoesqueleto até ao seu organelo alvo. A endocitose mediada por caveolae é o principal mecanismo através do qual os patógenos invadem uma célula e evitam a sua degradação nos lisossomas. As nanopartículas ao interagirem com a membrana induzem a formação de vesículas, que devido à ação da dinamina, destacam-se da membrana e, uma vez no citosol fundem-se com os caveosomas.

O objetivo do presente trabalho prendia-se em determinar qual a via de endocitose que as células da mama cancerígenas MDA-MB-231 utilizam para internalizar tanto micelas funcionalizadas como não funcionalizadas. Ao mesmo tempo, queríamos tentar perceber se o nanotransportador proposto protegeria o fármaco encapsulado da ação da P-gp. Havendo uma acumulação intracelular de salinomicina, esta poderia atuar sobre a proteína mesenquimal vimentina - dado o seu carácter tumorogénico - de forma a reduzir a sua expressão e, desta forma reduzir a capacidade de metastização destas células.

Para tal, o primeiro passo foi descobrir qual a concentração que mataria 50% das células, tanto para o fármaco livre como quando se encontrava encapsulado. Estes valores são 5.32 μM e 0.071 μM para a salinomicina encapsulada e livre, respetivamente, às 24 horas, e 51.94 μM e 5.34 μM para a salinomicina encapsulada e livre, respetivamente, às 48 horas. Os valores obtidos para a salinomicina livre estão dentro do intervalo de valores descrito na literatura para este fármaco.

Quando funcionalizadas as micelas induzem o aumento da expressão do recetor CD44, ao mesmo tempo que atrasam a entrada destas micelas em, pelo menos, 30 minutos. Ao contrário do descrito na literatura, tanto as micelas funcionalizadas como as não funcionalizadas têm as mesmas proteínas a intervir na sua internalização. Ou seja, as micelas não funcionalizadas são internalizadas por um processo mediado por caveolae, enquanto nas funcionalizadas há um recrutamento de caveolae para a membrana.

A P-gp pode estar localizada em muitos organelos celulares, como o retículo endoplasmático, o aparelho de Golgi e nos compartimentos endossomais. Quando as células estão em contacto com micelas vazias, a intensidade de fluorescência da P-gp não varia por comparação com o nível basal que esta proteína apresenta (controlo). Quando em contacto com micelas com fármaco encapsulado, verifica-se um aumento da intensidade da P-gp, que se encontra localizada predominantemente em vesículas endocíticas, numa resposta à libertação intracelular de salinomicina. Quando tratadas apenas com salinomicina, para além de um aumento da intensidade da P-gp, há também uma acumulação desta proteína em redor do núcleo.

Tanto a salinomicina livre como a salinomicina encapsulada induzem um aumento da expressão de vimentina o que, de acordo com a literatura, pode significar que a salinomicina fosforila a proteína Akt, levando à consequente fosforilação da vimentina, bloqueando a apoptose.

Desta forma, as células MDA-MB-231 utilizam a caveolina para internalizar estas micelas, sendo que a sua funcionalização induz um aumento da expressão do recetor CD44. Uma vez que na presença de micelas vazias não se verificou uma estimulação da atividade da P-gp, estas têm potencial para se tornarem bons nanotransportadores e permitir a acumulação intracelular de fármacos. No entanto a utilização de salinomicina poderá não ser uma boa terapia para erradicar estas células cancerígenas dado que induziu um aumento da expressão da vimentina.

Palavras-chave: Cancro da mama; CD44; P-glicoproteína; nanopartículas; endocitose

Contents

Agradecimientos.....	II
Abstract	III
Resumo.....	IV
Figures Index.....	VII
Tables Index	VIII
List of abbreviations.....	IX
1. Introduction	1
1.1. Breast cancer pathology	1
1.2. Cancer Stem Cells and Epithelial-to-Mesenchymal Transition	1
1.3. CD44 Receptor - A Stemness Marker for Breast Cancer Cells.....	2
1.4. P-glycoprotein – The first molecular obstacle in cancer treatment	4
1.5. Nanoparticles – A way to overcome P-glycoprotein action	5
1.6. Nanoparticle’s cellular Endocytosis	6
2. Objectives.....	7
3. Materials and Methods	8
3.1. Cell culture, cell seeding and cell viability assay	8
3.2. Polymeric nanoparticles functionalization and SDS-PAGE	8
3.3. Endocytosis assay and immunocytochemistry	8
3.4. P-glycoprotein assay and immunocytochemistry	9
3.5. Gene expression analysis: Drug treatment, cell lysis and total mRNA extraction	10
3.6. cDNA synthesis and quantitative PCR (RT-qPCR)	11
3.7. Statistical analysis	12
4. Results	13
4.1. In vitro cytotoxicity of free salinomycin and loaded micelles	13
4.2. Nanoparticles functionalization with CD44v6 antibody	14
4.3. Expression of endocytosis proteins after nanoparticle incubation	15
4.4. P-glycoprotein activity after incubation with loaded micelles and free salinomycin.....	18
4.5. Vimentin expression modulation.....	21
5. Discussion	23
6. Conclusion.....	26
7. References	27

Figures Index

Figure 1.3.1 – Schematic representation of membrane CD44 receptor. Being localized in lipid rafts its association with ezrin is restricted. Its extracellular domain, that contains the variable exons (represented in red) interacts with hyaluronan, while its intracellular domain interacts with ERM or Merlin. (Reproduced from Horta et al.,2010)	3
Figure 1.4.1 – Schematic representation of ATP-dependent transporter P-glycoprotein and its interaction with anticancer drugs. P-glycoprotein uses ATP to actively transport cytotoxic drugs from the cells. (Reproduced from Fu et al, 2013)	5
Figure 1.4.2 - Activation of multidrug resistance phenotype as an outcome of signaling pathways that result from the interaction of HA/CD44 with Nanog (I) and with ankyrin (II). (Reproduced from Bourguignon et al, 2008).....	5
Figure 4.1.1 - MDA-MB-231 cell viability after 24 and 48 hours of incubation with plain micelles (PM), loaded micelles (PM _{sal}) and free salinomycin (SAL) in five different concentrations ([50 µM]; [5 µM]; [0.5 µM]; [0.05 µM]; [0.005 µM]).	13
Figure 4.2.1 – 12% SDS-PAGE photography. This technique was used to evaluate the presence of free CD44v6 in the functionalized micelles dispersant phase. M1 – NZY colour protein marker I (molecular weight from 5 kDa to 245 kDa); PM ^{CD44} – functionalized plain micelles with CD44v6 ([5 mg/ml/5 µg/ml]); PM – plain micelles ([5 mg/ml]); CD44v6 – CD44v6 antibody used to functionalize the micelles ([5 µg/ml]); M2 – Protein Marker (All blue prestained protein standards, BioRad) (molecular weight from 10k Da to 250 kDa).....	14
Figure 4.3.1 – Immunofluorescence of CD44 receptor in MDA-MB-231 cells in three different conditions after 30 minutes of incubation at 37°C: Control – cells were incubated with culture medium; PM – cells were incubated with [1 µM] of plain micelles; PM ^{CD44} – cells were incubated with [1 µM] of functionalized plain micelles. Exposition time: 1500 ms. Scale bar: 50 µm.....	15
Figure 4.3.2 - Immunofluorescence of clathrin and CD44 receptor in MDA-MB-231 cells in three different conditions after 30 minutes of incubation at 37°C: Control – cells were incubated with culture medium; PM – cells were incubated with [1 µM] of plain micelles; PM ^{CD44} – cells were incubated with [1 µM] of functionalized plain micelles. Exposition time: 4000 ms for clathrin and 1500 ms for CD44. Scale bar: 100 µm.....	16
Figure 4.3.3 - Immunofluorescence of caveolin and CD44 receptor in MDA-MB-231 cells in three different conditions after 30 minutes of incubation at 37°C: Control – cells were incubated with culture medium; PM – cells were incubated with [1 µM] of plain micelles; PM ^{CD44} – cells were incubated with [1 µM] of functionalized plain micelles. Exposition time: 5500 ms for caveolin and 1500 ms for CD44. Scale bar: 100 µm.....	17
Figure 4.3.4 – Amplification of the merge from the double staining of CD44 receptor and caveolin proteins, where is evident a colocalization on certain membrane domains of CD44 receptor and caveolin proteins in MDA-MB-231 cells.	17
Figure 4.3.5 – Fluorescence intensity (a.u.) of CD44 receptor, caveolin and clathrin in three different conditions after 30 minutes of incubation: Control – cells were incubated with culture medium; PM – cells were incubated with [1 µM] of plain micelles; PM ^{CD44} – cells were incubated with [1 µM] of functionalized plain micelles. Values represent the mean ± SD for each 13 measurements. (*p≤0.05).	18
Figure 4.4.1 - Immunofluorescence of P-glycoprotein in MDA-MB-231 cells in three different conditions after 30 minutes of incubation at 37°C: Control – Cells were incubated with culture medium; PM – Cells were incubated with [1 µM polymer] of plain micelles; PM _{sal} – Cells were incubated with	

[1 μM polymer/0.68 μM_{sal}] of loaded micelles; and SAL – Cells were incubated with [0.68 μM_{sal}] of free salinomycin. Exposition time: 1500 ms. Scale bar: 50 μm 19

Figure 4.4.2 - Immunofluorescence of P-glycoprotein in MDA-MB-231 cells in three different conditions after 1 hour of incubation at 37°C: Control – Cells were incubated with culture medium; PM – Cells were incubated with [1 μM polymer] of plain micelles; PM_{sal} – Cells were incubated with [1 μM polymer/0.68 μM_{sal}] of loaded micelles; and SAL – Cells were incubated with [0.68 μM_{sal}] of free salinomycin. Exposition time: 1500 ms. Scale bar: 50 μm 20

Figure 4.4.3 - Fluorescence intensity of P-glycoprotein in three different conditions after 30 minutes and 1 hour of incubation at 37°C: Control – Cells were incubated with culture medium; PM – Cells were incubated with [1 μM polymer] of plain micelles; PM_{sal} – Cells were incubated with [1 μM polymer/0.68 μM_{sal}] of loaded micelles; and SAL – Cells were incubated with [0.68 μM_{sal}] of free salinomycin. Values represent the mean \pm SD of each thirteen measurements. (* $p \leq 0.05$; **** $p \leq 0.0001$). 21

Figure 4.5.1 - RT-qPCR analysis performed in total mRNA isolated from MDA-MB-231 cells after 48 and 72 hours treatment with [0.05 μM] and [1 μM] of plain micelles (PM), loaded micelles (PM_{sal}) and free salinomycin (SAL). Relative vimentin mRNA levels are normalized to the expression of β -actin mRNA of each experiment. Values represent the mean \pm SD of each duplicate of the experiment. (* $p \leq 0.05$). 22

Tables Index

Table 4.1.1 – IC50 values (μM) for free salinomycin (SAL) and loaded micelles (PM _{sal}) for 24 hours and 48 hours of incubation in MDA-MB-231 cells.....	14
Table 3.6. 1 - Amplification program used to synthesize cDNA	11
Table 3.6. 2 - Sequences of the primers used to amplified vimentin and β -actin.	11
Table 3.6. 3 - Amplification program used in Real-Time qPCR.....	11

List of abbreviations

ACRYL/BIS 29:1 – Solution of 38.67% (w/v) acrylamide and 1.33% (w/v) bis-acrylamide for a monomer to cross-linker ratio of 29:1

AKT – Also known as protein kinase B

ALDH1 – Aldehyde dehydrogenase 1

APS – Ammonium Persulfate

a.u. – Arbitrary units

BSA – Bovine Serum Albumine

CCB R-250 – Coomassie Brilliant Blue R-250

DMEM – Dulbecco's Modified Eagle's Medium

EEA1 – Early endosome antigen 1

EMT – Epithelial-to-mesenchymal transition

ERM – Ezrin, Radixin and Moesin protein family

FBS – Fetal Bovine Serum

PFA – Paraphormaldehyde

HA- Hyaluronan (or hyaluronic acid)

Hook1 – Protein Hook homolog 1

MAPK – Mitogen-activated protein kinase

MDR1 – Multidrug resistance (MDR) protein 1

MMP- Metalloproteinases

MMTV-PyV mT (transgene)- has the mouse mammary tumor virus (MMTV) long terminal repeat upstream of a cDNA sequence encoding the Polyoma Virus Middle T antigen (PYVT)

mTOR – Mechanistic target for rapamycin

MTT – 3-(4,5-dimethylthiazol-2-yl) -2,5-diphenyltetrazolium bromide

NP - Nanoparticles

Pen Strep – Penicilin Streptomycin

P-gp – P-glycoprotein

PI3K – Phosphatidylinositol-4,5-biphosphate 3-kinase

p53 – Tumor protein 53

SD – Standard Deviation

SDS-PAGE – Sodium dodecyl sulphate polyacrylamide gel electrophoresis

SOX2 – (Sex determining region Y)-box 2 transcription factor

Stat-3 – Signal transducer and activator of transcription 3

TNBC – Triple-Negative Breast Cancer

TGF- β – Transforming growth factor beta

TG-SDS – Buffer solution of Tris base, Glycine and Sodium Dodecyl Sulfate

1. Introduction

1.1. Breast cancer pathology

The human breast is mainly composed of connective and adipose tissue, that comprises 12 to 20 lobes (sections), each containing the epithelial components - lobules and ducts, that are responsible for producing the milk and carry it to the nipple, respectively - and the stroma composed of fibroblasts, endothelial, adipocytes and hematopoietic cells. In the case of the male breast, the lobules are undeveloped as there is no physiological condition for it to produce milk¹⁻³.

The ducts contain luminal cells (divided into ductal and alveolar cells that limit the ducts and linger through pregnancy) and myoepithelial cells (basal and contractile cells that drive the milk from the lobules to the nipple¹⁻³). The modifications that happen to the breast cells during pregnancy suggest the existence of cells with high regenerative and proliferative capabilities, all associated with stem cells³.

Breast cancer can be divided into two main groups – carcinomas and sarcomas. Carcinomas are the type of cancers that originate from the epithelial components and, in the case of the breast, corresponds to the epithelium that line the lobules and the ducts. Around 80% of breast cancers originate in the ductal region and about 20% in the lobules. Sarcomas correspond to cancers that originate in the stromal components of the breast, and account for 1% of all cases of breast cancer, being the rarest type of breast cancer¹.

To estimate the breast cancer's stage pathologists, rely on the accurate quantification of specific biomarkers either for prognostic and/or as predictive tools. Predictive biomarkers, such as estrogen receptor (ER) and progesterone receptor (PR), elucidate to which extent a patient will respond to a given therapy. Prognostic biomarkers, such as HER2, relate to the patient's overall clinical outcome, i.e., their presence or absence are indicative of the risk of recurrence and mortality¹.

However, oncologists and investigators are more focused in the triple-negative breast cancer (TNBC) adenocarcinomas which lack all the biomarkers described above and presents a poor prognosis and aggressive clinical behavior, since they do not respond to hormonal therapies and treatments targeted against among others, HER2 receptors⁴⁻⁶. Due to their molecular heterogeneity TNBC can be divided into five subtypes: Basal-like; Mesenchymal; Mesenchymal-like; Immunomodulatory and Luminal AR⁷.

Basal-like cancers have their cell cycle and DNA repair mechanisms' activity increased, which translates into a higher rate of cell proliferation. Mesenchymal and mesenchymal-like ones develop mechanisms that contribute to the epithelial-to-mesenchymal transition (such as PI3K/AKT and mTOR pathway), but mesenchymal-like cancers have a decreased expression of proliferating genes. The so called immunomodulatory cancers have an increased expression of genes involved in cytokine signaling and core immune transduction mechanisms - NF- κ B and JAK/STAT pathways. Finally, in luminal AR cancers, hormonal pathways and androgen/estrogen metabolic pathways are expressed differently when compared with the other subtypes^{7,8}. Of all the subtypes described above our work will focus on the mesenchymal-like subtype, since they can exhibit a stem-like phenotype. This cell population can generally be designated as cancer stem cells.

1.2. Cancer Stem Cells and Epithelial-to-Mesenchymal Transition

Cancer stem cells (CSCs) or cancer initiating cells (CICs) are characterized for their ability to reconstitute the initial tumor heterogeneity owing their self-renew and differentiation ability⁹⁻¹². However, since these cells have a low proliferating rate, or have a high quiescent status, the utilization

of cytotoxic anticancer agents against these cells is useless because they mostly kill proliferating cells. That is the main reason patients who have an intrinsic resistance to the anticancer therapy exhibit an elevated number of stem-like cells^{9,11,12}. Therefore, it is critical to discover new therapies that selectively target this population of cancer cells^{11,12}.

Breast cancer stem cells diverge from the remaining cancer cells because they overexpress some surface markers, such as CD44, while downregulate other, such as CD24^{13,14}. CD44 is the widely used stemness marker and in our opinion it has the potential to become a biomarker in cancer therapy¹⁵.

Cancer cells can also undergo epithelial-to-mesenchymal transition (EMT). There are three types of EMT: type 1 occurs during embryo development; type 2 during tissue regeneration; and type 3 during cancer metastasis, the latter being the one we are interested in. Epithelia is a well-organized group of cells all tight up due to cell-cell junctions. In order to become mesenchymal cells, tight junctions and adherens junctions are destroyed and E-cadherin is degraded and downregulated. While epithelial genes are suppressed, mesenchymal protein genes are activated and the cells' cytoskeleton is reorganized in order to promote migration and invasion¹⁶.

One of the mesenchymal proteins is vimentin. It is a 57 kDa intermediate filament whose function is dependent on its phosphorylation and de-phosphorylation dynamics^{17,18}. Vimentin is essential in the endocytic pathway, namely, in the late endocytic traffic mechanisms¹⁸ as well as to maintain tissue/cellular integrity¹⁷. In leukocytes it has been shown that vimentin participates in the PI3K/AKT signaling pathway as a downstream effector of PI3K^{19,20}. Zhu *et al.* (2011), demonstrated that caspase-induced apoptosis in soft-tissue sarcoma (STS) can be blocked by vimentin upon phosphorylation mediated by AKT1. On the contrary, the inhibition of AKT1 leads to proteolysis of vimentin, and eventually all the morphological alterations of a dead cell²¹.

In melanoma cells, Alonso *et al.* (2014), discovered that Rab7 expression is selectively regulated in highly invasive melanoma cells, and due to its role in regulating vesicle trafficking Rab7 can modulate the levels and/or localization of pro-tumorigenic proteins²². Rab7 also regulates cell's motility through its interaction with Rac1 and vimentin. As stated by Margiotta *et al.* (2016), depletion of Rab7 leads to a lower migration rate since it interferes with Rac1 activity, resulting in a decrease of vimentin phosphorylation and assembly²³.

1.3. CD44 Receptor - A Stemness Marker for Breast Cancer Cells

CD44 is a transmembrane glycoprotein, encoded by 20 exons, that can have a size range from 80 to 200 kDa resulting from alternative splicing and posttranslational modifications, such as glycosylation and palmitoylation²⁴. These modifications are responsible for the transition from the "inactive" state (low binding affinity) to the "active" state (high binding affinity)²⁵.

The most expressed and small form of CD44 is its standard isoform (CD44s)²⁶, which only have the constant exons (exons 1-5 and exons 16-18). Insertion of the variable exons (exons 6-15 and exons 19-20) creates larger isoforms and additional binding sites, and their expression is dependent on the extracellular microenvironment and type of tissue^{24,27}. Whereas the standard isoform is expressed in all cell types, the variant isoforms (CD44v) are expressed in cells that underwent unique alterations¹⁵.

CD44 receptor is composed of an extracellular domain, a transmembrane domain and an intracellular domain (*Figure 1.3.1*)¹⁵. The extracellular domain regulates the interaction with the extracellular matrix during cellular migration in an environment with high concentration of hyaluronan^{26,28}. This domain can be proteolytic cleavage, by metalloproteinases, leaving the transmembrane domain of the receptor intact and soluble CD44, that corresponds to the extracellular domain²⁹. It can be prompt by extracellular calcium influx, proteinase kinase C (PKC) activation, Rho

family small GTPases, Ras and Rac oncoproteins activation²⁸. Thomas *et al.* (1993), proposed that this soluble CD44 could act as a competitive antagonist of endogenous HA that when bound with CD44 receptor triggers a cascade of mechanism that result from the interaction CD44-HA³⁰.

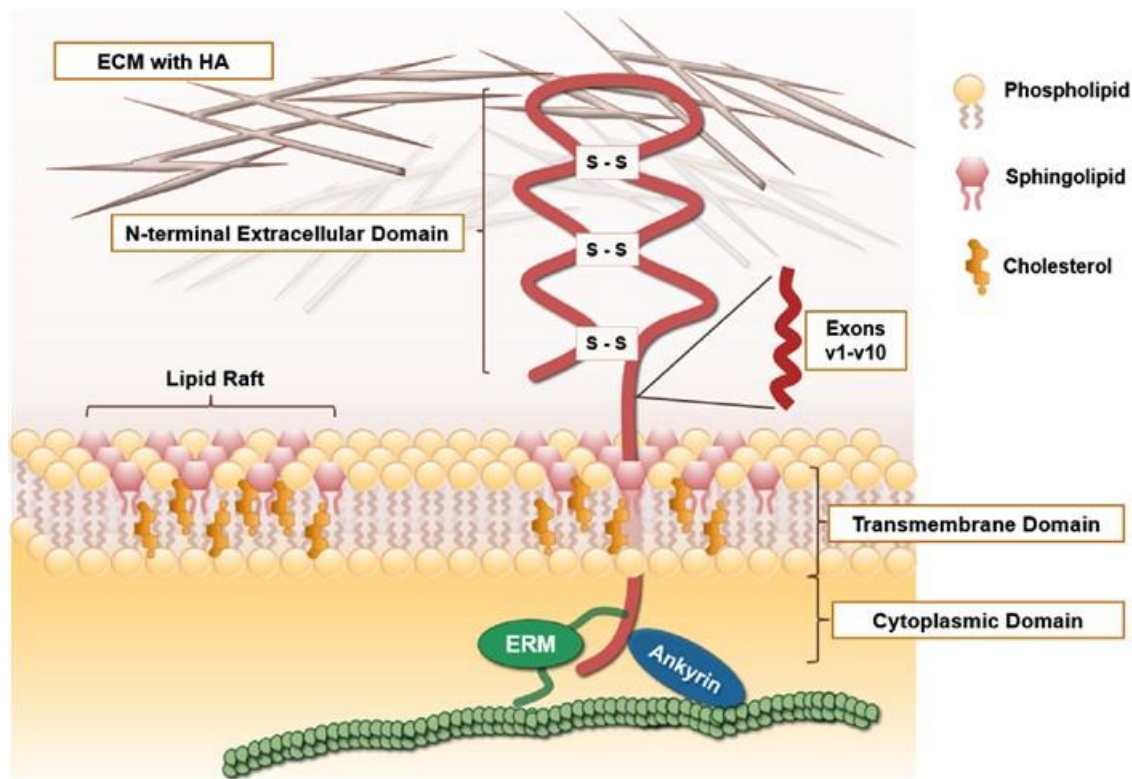


Figure 1.3.1 – Schematic representation of membrane CD44 receptor. Being localized in lipid rafts its association with ezrin is restricted. Its extracellular domain, that contains the variable exons (represented in red) interacts with hyaluronan, while its intracellular domain interacts with ERM or Merlin. (Reproduced from Horta *et al.*, 2010)

The cleavage of the extracellular domain induces the proteolytic cleavage of the intact fraction of the receptor, by presenilin-dependent γ -secretase²⁸, generating two fragments with approximately 25 kDa – corresponding to the C-terminal fragment (CTF) - and 12 kDa - corresponding to the intracellular domain (CID) of the receptor. This last fragment can translocate to the nucleus activating transcription of the CD44 gene itself^{26,29} and more important the Twist transcription factor³¹.

CD44 receptor is mainly localized in the membrane lipid rafts which, according to Babina *et al.* (2014), limits its association with ezrin at the same it limits the migration in normal cells. Decrease in CD44's palmitoylation levels leads to its translocation to a non-raft fraction of the membrane where it binds with oncogenic proteins to stimulate cell migration³². This indicates that palmitoylation controls the “dispersion” of CD44 receptors in the various membrane domains and, possibly, its association with ERM (ezrin, radixin and moesin) proteins^{26,33}.

ERM competes with Merlin for the binding sites in the cytoplasmic tail of CD44 receptor (*Figure 1.3.1*). Namely, if there is a high cellular density Merlin binds to CD44 and ERM no longer binds, attaining an inhibition of Ras-dependent cellular growth. On the contrary, when Merlin is phosphorylated and, consequently, deactivated by p21-associated kinase (PaK2), it leaves binding spaces in CD44's cytoplasmic tail empty to which ERM is able to bind and thus promote cytoskeleton reorganization and cellular invasion²⁴.

Apart for being a co-receptor for growth factors and cytokines cell uptake¹⁵, CD44's interaction with constituents of the extracellular matrix (such as HA) triggers several intracellular mechanisms that

sustains cell's survival, proliferation and invasion (by activation of Rho GTPases)^{25,32}, promoting also the reorganization of the cytoskeleton²⁴.

One of these mechanism is strictly related with tumorigenic pathways activation, such as PI3K/Akt and MAPK-Ras signaling, and further interaction with tyrosine kinases³⁴ and recruitment of adaptor proteins that bind to the cytoplasmic tail²⁴. The other is downregulation of apoptosis and stabilization of MDR1 receptor³⁴. In T-cell acute lymphoid leukemia and adult T-cell lymphoma, expression of CD44 is associated with acquisition of drug resistance and an enhancement of drug efflux²⁷.

The PI3K/Akt pathway has an important role in EMT, where Akt is a downstream signaling effector of CD44s. By using MCF10A cells, Brown *et al.* (2011) demonstrated that the dynamic of alternative splicing of CD44v isoforms to CD44s, induced by TGF- β or Twist, is a key element for cells to undergo EMT³⁵.

As proved by Meilgo *et al.* (2004), cells expressing CD44 variant isoforms, more specifically CD44v6 and CD44v9, are not affected by Fas-mediated apoptosis, acting as a pro-survival signal. They proposed that the extracellular domain of CD44 receptor interacts with the Fas receptor, colocalize in lipid rafts, inhibiting the binding of FasL and the consequent activation of Fas signaling³⁶. Interestingly hyaluronan can activate caspase-3-depedent apoptosis, at the same time that it can inhibit PI3K/AKT signaling pathway²⁴.

When tumor suppressor p53 binds to CD44 promotor it represses its transcription and the cell can respond to stress induced signals by apoptosis activation, and in the absence of p53 there is an increased expression of CD44 and inhibition of apoptosis²⁴.

The high levels of CD44 receptor illustrate the rapid recycling pathway this receptor undergoes during metastasis and development. According to Maldonado *et al.* (2013), CD44 contains a sorting signal that allows it to avoid EEA1-associated endosomes and the further pathway to lysosomes, and by action of Hook1 and Rab22 is rapidly sorted out in tubular recycling endosomes³⁷.

Despite all the events mention above, CD44 receptor can also function as a keeper against metastasis and invasion. When crossing an MMTV-PyV mT mice with a CD44 knock-out mice, Lopez *et al.* found that CD44 absence resulted in an increased metastatic potential, and the ability of breast cancer cells expressing CD44 receptor to migrate to hyaluronan-enriched microenvironment is blocked³⁸.

Overall during mitosis, activation of the CD44 receptor leads to the rupture of intracellular junctions, separating cells from one another, and from the surface to which they are attached (CD44-HA)³⁴.

1.4. P-glycoprotein – The first molecular obstacle in cancer treatment

One of the most important obstacles (nano)drugs encounter once they reach the tumor cells is the membrane efflux P-glycoprotein (P-gp) (*Figure 1.4.1*). This 170 kDa ATP-dependent surface transporter exists in membrane surfaces of all cells, being overexpressed in cancer cells and responsible for the efflux of all anticancer drugs. P-gp can transport both cytotoxic drugs, neutral, amphiphilic and cationic molecules against their concentration gradient³⁹⁻⁴¹.

When the hydrophobic substrates, such as salinomycin, interact with the transmembrane domain of P-gp, they are ejected from the cytoplasm preventing their cytosolic accumulation and their pharmacological activity on the intended intracellular target, conferring to these cells a multidrug resistance phenotype³⁹⁻⁴¹. Multidrug resistance is the mechanism used by cancer cells to become

insusceptible to one drug, and consequently other drugs, which have different mechanisms of action in these cells³⁹.

Salinomycin is a potassium ionophoric therapeutic drug that targets cells expressing high levels of mesenchymal proteins, i.e., breast cancer stem cells. Its activity is 100 folds higher than paclitaxel. By inhibiting P-gp activity, salinomycin restores cancer cells' sensitivity to other therapeutic drugs. Salinomycin can also induce autophagy and increase the expression level of p53 protein and interfere with angiogenesis since it reduces the expression of fibronectin, important to elongate the blood vessels^{11,12,42}. According to An *et al.* (2015), salinomycin downregulates cyclin D1 and induces DNA damage, suppressing the formation of mammospheres and lowering tumor growth by downregulating CD44 and ALDH1, two of cancer stem cells markers⁴³.

When HA binds to CD44 receptor (*Figure 1.4.2*) it activates the transcription factor Nanog that can actively

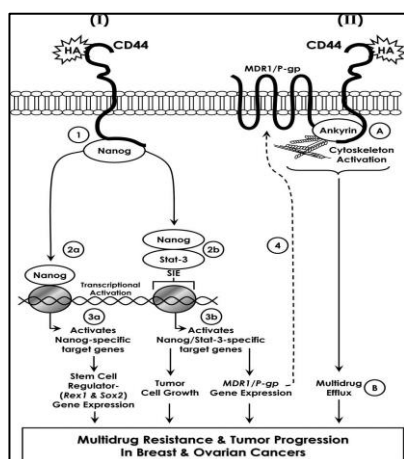


Figure 1.4.2 - Activation of multidrug resistance phenotype as an outcome of signaling pathways that result from the interaction of HA/CD44 with Nanog (I) and with ankyrin (II). (Reproduced from Bourguignon *et al.*, 2008)

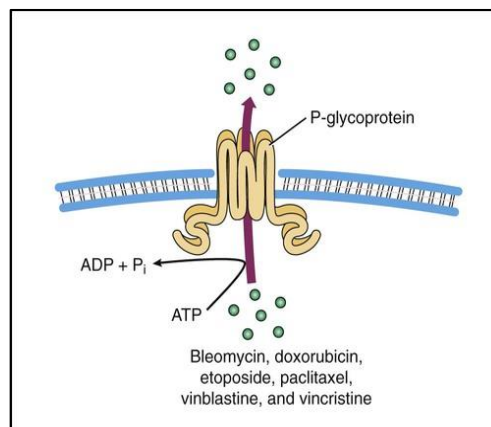


Figure 1.4.1 – Schematic representation of ATP-dependent transporter P-glycoprotein and its interaction with anticancer drugs. P-glycoprotein uses ATP to actively transport cytotoxic drugs from the cells. (Reproduced from Fu *et al.*, 2013)

transcript its target genes, such as Sox2, or complexes with Stat-3, leading to the activation and overexpression of MDR1 gene (P-glycoprotein), at the same time that protein ankyrin binds to P-gp receptor, enhancing the drug efflux and tumor progression, specifically in breast and ovarian cancers^{34,44}. According to Bourguignon *et al.* (2008), the inability to enroll ankyrin and P-gp to form a complex with CD44 results in a decrement of active drug efflux and, therefore, decreases multidrug resistance (mediated by CD44) and enhances the sensibility of cancer cells to therapies⁴⁴. González *et al.* (2005), found out that P-gp and CD44 colocalize within the cell membrane of MDR cells, and that when disturbed it affects drug resistance as well as cell migration and invasion⁴⁵.

Recycling, degradation and transport trafficking of transmembrane P-gp is regulated by Rab4 and Rab5. It is suggested that Rab4 is responsible for P-gp's exocytosis from early endosomes, while Rab5 regulates both endocytosis and exocytosis of P-gp, serving as a mean to control its expression on the membrane⁴¹.

1.5. Nanoparticles – A way to overcome P-glycoprotein action

The ideal anticancer drug would be highly specific and efficient against cancer cells, have lower systemic toxicity and high levels of biocompatibility, a high concentration of the drug in the site of the tumor, all the while preventing drug degradation and undesirable effects^{46,47}. Nanocarriers (nanoparticles - NP) are being developed to become this so called ideal drug. The efficiency of these carriers depends on several factors, namely, their size, surface charge and surface functionalization, as they regulate the interactions of these NP with the cellular membrane and membrane internalization in the targeted cells^{47–}

Nanocarriers are nanometer systems composed of at least two components, where one of them is the active agent and the other is responsible for protecting this agent and transporting it⁵⁰ while increasing drug's circulation period⁴⁸. One example of these type of carriers are polymeric micelles. Micelles are mainly composed of a hydrophobic polymeric chain core and a hydrophilic polymeric shell corona⁴⁶. This project was developed using poloxamer-based micelles to deliver (and protect) salinomycin - as an anti-cancer agent, against breast cancer stem cells.

Nanocarriers biologic interaction can occur through two different approaches that dependent on their physical-chemical properties – passive targeting and active targeting⁵⁰.

Passive targeting takes advantage of the cancer's characteristics such as immature vasculature, imbalance lymph drainage and consequently, NP become entrapped, in a so called EPR (Enhanced Permeabilization and Retention) effect, so that NP (size range between 10-200 nm) can enter and accumulate in solid tumors. Active targeting is a more complex mechanism that for NP just occurs upon passive targeting. Once in the tumor microenvironment functionalized NP specifically target an overexpressed protein/receptor on the membrane surface of cancer cells⁵⁰.

Functionalized NP are decorated with proteins, antibody or antibodies fragments, specific for a surface (over)expressed receptor/protein. This system add value relies on enhanced target specificity. Moreover, the “stealth” NP can circulate in the body for longer periods when compared to the free drug, without being recognized/eliminated by the reticuloendothelial system (RES)⁴⁹. The mechanism by which functionalized and non-functionalized particles enter the cell is expected to involve different molecules.

1.6. Nanoparticle's cellular Endocytosis

Endocytosis is the process by which cells can intake macromolecules, such as proteins, that cannot cross the membrane due to their physical properties. It is also the main entrance of particles into the cells. It can be divided into pinocytosis and phagocytosis⁵¹, being the later the process by which particles in the range size of micrometers are endocytosed by phagocytic cells and cleared from the bloodstream⁵¹⁻⁵³. In this case “debris” are covered by the circulate opsonins making them recognizable by the cell membrane receptors macrophages⁵¹.

Clathrin- and caveolae-mediated endocytosis are the most studied players related to the particles internalization, mainly NP⁵⁴. According to Rejman *et al.* (2004), NP with a diameter higher than 200 nm enter the cell through caveolae-mediated endocytosis, while with a diameter under 200 nm the chosen pathway is clathrin-mediated endocytosis⁵⁵. NP with a size of 10 nm first accumulate on the membrane and then are endocytosed, whereas larger NP are directly internalized^{53,56}.

Clathrin-dependent endocytosis has been extensively studied receptor-mediated endocytosis mechanism⁵⁴. It can have an important role in signaling downregulation through receptor internalization and degradation and in maintenance of homeostasis. Poly(ethylene glycol)-Polylactide, silica-based and poly(lactic-co-glycolic acid) (PLGA) NP are just a few examples of nanocarriers that are uptaken by clathrin-mediated endocytosis⁵⁷.

Wherever a functionalized NP binds to a specific membrane receptor, forming the nanoparticle-receptor complex, endocytic proteins are recruited, including AP2 and clathrin, to form the clathrin-coated pit (CCP). The vesicle containing the NP, detach from the membrane through the GTPase activity of protein dynamin, forming the clathrin-coated vesicle (CCV). Once inside the cells, the clathrin coat is degraded in the cytosol and the vesicle move along the cytoskeleton (involving actin) towards their destination, depending on the type of receptor they bind to⁵⁸.

Caveolae-mediated endocytosis is the main mechanism involved in pathogens cell infection to avoid lysosomal degradation^{58,59}. This type of internalization depends on cholesterol-enriched membrane domains, such as lipid rafts and caveolae⁶⁰. The main component of caveolae is the presence of a hairpin-like protein called caveolin-1 which segregate ligands and their downstream effector in close proximity for signal activation and transduction. Nanocarriers such as quantum-dots and polysiloxane NP are uptaken by a caveolae-mediated process⁵⁷.

When NP interact with the membrane surface, they induce the formation of vesicles, that due to the action of protein dynamin are disconnected from the membrane, and once inside the cell they fuse with caveosomes (neutral pH), further progressing to the early endosomes. Just like clathrin-mediated internalization, this type of internalization requires actin and microtubules to move the vesicles all over the cell⁶¹.

2. Objectives

Knowing that nanocarriers preferably enter the cell via endocytosis this project main goal was to evaluate which type of endocytosis is used when the drug is carried by polymeric micelles (functionalized and non-functionalized). With this intend MDA-MB-231 breast cancer cells were selected as a disease model since they are mesenchymal-like cells and highly invasive, and considering they express high levels of mesenchymal markers such as vimentin.

A decrease in this cell marker expression would mean that the metastatic potential is impaired and, eventually, their mesenchymal-like phenotype could be reverted to an epithelial-like. This could be accomplished with the proposed salinomycin loaded micelles. At the same time, we also wanted to know if the type of polymer used to make these particles would conceal salinomycin to P-gp's activity.

3. Materials and Methods

3.1. Cell culture, cell seeding and cell viability assay

Triple-negative breast cancer cell line MDA-MB-231 (ATTC, USA) was maintained in Advanced DMEM (BioWhittaker; BE12-709F) with 10 % FBS (BioWest; S181BH-500), 1% GlutaMax-I (100X) (Life Technologies; 35050061); and 1% Penicillin and Streptomycin (Life Technologies; 15140-122).

For immunocytochemistry, glass coverslips and wells were washed with 70% ethanol prior to seeding for enhanced cell adhesion. For immunocytochemistry, 50,000 cells/well were seeded in 24-well plates, and 250,000 cells/well were seeded in 6-well plates for mRNA extraction.

For cell viability assays, 10,000 cells/well were used in a 96-well plate. 24 hours after seeding, the medium was removed and washed with 100 μ l of 1x PBS (VWR; Portugal). The experimental conditions comprised plain micelles, loaded micelles and free salinomycin in five different concentrations – [50 μ M]; [5 μ M]; [0.5 μ M]; [0.05 μ M]; [0.005 μ M] - and incubated for 24 hours and 48 hours. By the end of this time, the medium was removed and each well was washed with 1x PBS. Cell viability was characterized by the MTT assay. Briefly, cells were incubated for 3 hours with MTT solution ([0.5 mg/ml] non-supplemented medium/well) (VWR; Portugal) and then lysed with DMSO (VWR; Portugal) and absorbance (570 nm) was measured with FLOUstar Omega MicroPlate Reader. Results were analyzed with GraphPad Prism software.

3.2. Polymeric nanoparticles functionalization and SDS-PAGE

To functionalize micelles, a stock solution of plain micelles formulation ([10 mg/ml]) was added to a microtube and combined with CD44v6 antibody ([0.5 mg/ml]) (Life Technologies; 336700), to obtain a final antibody concentration of [5 μ g/ml]. These two components were incubated overnight with a 10-rpm stirring, at room temperature and protected from light.

To evaluate the integrity of CD44v6 antibody after functionalization a SDS-PAGE was performed. The first step was to make a 12% resolving and a 4% stacking gel. Sample loading buffer (5x) (NZYTech; MB11701) was added to each sample and boiled for 5 minutes at 95°C to denature proteins, allowing its separation by their molecular weight. Electrophoretic separation, using 1x TG-SDS running buffer (AMRESCO; M148-4L), was performed at 150 V for 1h 30 min using Mini-PROTEAN Tetra Vertical Electrophoresis Cell and PowerPac Basic Power Supply, BioRad. To stain the polyacrylamide gel, the manufacturer's instructions were followed. Briefly, the gel was washed 3 times (5 minutes each) with deionized water, removing all traces of water before adding the Coomassie brilliant blue R-250 (CBB R-250) (BioSciences; 786-498). CBB R-250 was incubated with the gel for 1 hour at room temperature. Lastly, the gel was washed 3 times with deionized water.

3.3. Endocytosis assay and immunocytochemistry

To study the interactions between micelles and endocytic proteins, cells were incubated with [1 μ M polymer] of functionalized and non-functionalized plain micelles for 30 minutes. Prior to staining cells were fixed with 4% PFA (MERCK; 104005) for 15 minutes, at room temperature, and washed with 1x PBS (VWR; Portugal).

When double-staining for clathrin/CD44 and caveolin/CD44, cells were permeabilized with 0.5% Triton X-100 (MERCK; 112298) for 30 minutes, at room temperature and washed with 1x PBS. Cells were then blocked with 1% BSA (Sigma Aldrich; A3912) for 1 hour, at room temperature, and washed with 1x PBS. Cells were incubated with primary antibody diluted in 1% BSA, according with the optimized concentration and incubation time (*Table 3.4.1*) and washed with 1x PBS. Then were incubated with secondary antibody diluted in 1% BSA, in the optimized concentration and incubation time (*Table 3.4.1*).

When staining CD44 receptors, cells were permeabilized with 0.1% Triton X-100 (MERCK; 112298) for 30 minutes, at room temperature and washed with 1x PBS. Then they were blocked with 1% BSA for 1 hour, at room temperature, and washed with 1x PBS. Incubation for 45 minutes, at room temperature with primary antibody, diluted in 1% BSA (*Table 3.4.1*) and washed with 1x PBS. Incubation with the same quantity of secondary antibody, diluted in 1% BSA (*Table 3.4.1*), for 30 minutes, at room temperature.

Cells were then washed with 1x PBS, and counterstained with DAPI (Life Technologies; D3571), diluted in 1x PBS (1:1000) for 20 minutes, at room temperature. Coverslips were washed in 1x PBS, followed by cold methanol (Sigma Aldrich; 32213), and then mounted in DPX mounting medium (MERCK; 100579). All samples were visualized with Zeiss Microscope and analyzed with ImageJ.

3.4. P-glycoprotein assay and immunocytochemistry

For P-glycoprotein assay cells were incubated with [1 μ M polymer] of plain micelles, [1 μ M polymer/ 0.68 μ M_{sal}] of loaded micelles and [0.68 μ M_{sal}] of free salinomycin in non-supplemented medium, for 30 minutes and 1 hour. Cells were fixed with 4% PFA (MERCK; 104005) for 15 minutes, at room temperature, and washed with 1x PBS (VWR; Portugal).

When staining P-glycoprotein, cells were permeabilized with 0.1% Triton X-100 (MERCK; 112298) for 30 minutes, at room temperature and washed with 1x PBS, and then blocked with 1% BSA for 1 hour, at room temperature, and washed with 1x PBS. Incubation for 45 minutes, at room temperature with primary antibody, diluted in 1% BSA (*Table 3.4.1*) and washed with 1x PBS. Incubation with the same quantity of secondary antibody, diluted in 1% BSA (*Table 3.4.1*), for 30 minutes, at room temperature.

Cells were then washed with 1x PBS, and counterstained with DAPI (Life Technologies; D3571), diluted in 1x PBS (1:1000) for 20 minutes, at room temperature. Coverslips were washed in 1x PBS, followed by cold methanol (Sigma Aldrich; 32213), and then mounted in DPX mounting medium (MERCK; 100579). All samples were visualized with Zeiss Microscope and analyzed with ImageJ.

Table 3.4.1 - List of antibodies used in immunocytochemistry with the optimized dilution and incubation time.

	Antibody name	Supplier	Catalog number	Dilution	Incubation time
CD44 Staining	CD44 anti-mouse (156-3C11) monoclonal antibody	Life Technologies	MA5-13890	1:100	Overnight
	F(ab') ₂ -Goat anti-mouse IgG (H+L) Secondary antibody, FITC	Life Technologies	A24513	1:500	1 hour
	CD44 antibody (19H8L4), ABfinity Rabbit monoclonal	Life Technologies	701406	1:100	45 minutes
	F(ab') ₂ -Goat Anti-Rabbit IgG (H+L) Secondary antibody, TRITC	Life Technologies	A24536	1:500	30 minutes
Caveolin Staining	Caveolin-1 Anti-Rabbit Antibody	Cell Signaling	3238	1:100	Overnight
	F(ab') ₂ -Goat Anti-Rabbit IgG (H+L) Secondary antibody, TRITC	Life Technologies	A24536	1:500	1 hour
Clathrin Staining	Clathrin Heavy Chain (P1663) Anti-Rabbit Antibody	Cell Signaling	2410	1:200	Overnight
	F(ab') ₂ -Goat Anti-Rabbit IgG (H+L) Secondary antibody, TRITC	Life Technologies	A24536	1:500	1 hour
P-gp Staining	Anti-P-Glycoprotein mouse monoclonal antibody (C219)	MERCK	517310	1:200	1 hour
	Goat anti-mouse IgG (H&L) Alexa Fluor 594 (Secondary antibody)	Abcam	Ab150120	1:500	30 minutes

3.5. Gene expression analysis: Drug treatment, cell lysis and total mRNA extraction

To ascertain whether salinomycin would interfere with vimentin expression 24 hours after seeding cells were incubated with [0.05 μ M] and [1 μ M] of plain micelles, loaded micelles and free salinomycin, and incubated for 48 hours and 72 hours, at 37°C. After the incubation time, cells were harvested by washing each well with 1x PBS (VWR; Portugal) and then scrapping in lysis solution (50 mM Tris-HCl; 150mM NaCl; 5% Glycerol; 0.5% Triton X-100; H₂O).

The lysate was transferred to a 1.5 ml Eppendorf tube and stored at -80°C, overnight. Once defrosted, lysates were centrifugated for 2 minutes at maximum speed and 50 μ l of supernatant was

transferred to a new 1.5 ml Eppendorf tube for total mRNA isolation. RNA extraction was performed with NZY Total RNA isolation Kit (NZYTech; MB13402).

3.6. cDNA synthesis and quantitative PCR (RT-qPCR)

cDNA was synthesized using NZY First-Strand cDNA Synthesis Kit (NZYTech; MB12501), according to the manufacturer's instruction, starting from 1 µg of RNA as a template. cDNA was synthesized following amplification program in *Table 3.6.1*, performed in Multi Gene II Thermal Cycle (Labnet; USA).

Real-time PCR was performed in ABI Prism 7300 Sequence Detection System (Applied Biosystem by Life Technologies, USA), using SybrGreen Master Mix (2x), ROX plus (NZYTech; MB21901), and [1 µM] of specific primers for the genes of interest (vimentin: primers #1 and #2; endogenous control – β-actin: primers #3 and #4) (STAB VIDA; Portugal) (*Table 3.6.2*) and 1µl of RNase free water (NZYTech; MB11101). The amplification program used is described in *Table 3.6.3*. Technical triplicates from each experiment, and duplicates from each sample were assessed in all cases. Quantitative analysis was performed using the relative standard curve method ($\Delta\Delta C_t$, Applied Biosystems by Life Technologies™, USA).

Table 3.6.1 - Amplification program used to synthesize cDNA

Temperature (°C)	Time (min)
65	5
25	10
50	50
85	5
4	∞

Table 3.6.2 - Sequences of the primers used to amplified vimentin and β-actin.

Primers	Sequence (5'→ 3')
Vimentin forward (#1)	CGGGAGAAATTGCAGGAGGA
Vimentin reverse (#2)	AAGGTCAAGACGTGCCAGAG
β-actin forward (#3)	ACAGAGCCTCGCCTTTGCC
β-actin reverse (#4)	GATATCATCATCCATGGTGAGCTGG

Table 3.6.3 - Amplification program used in Real-Time qPCR.

Temperature	Time	Step
95°C	10 min	Holding Stage
95°C	15 sec	Cycling Stage (40 cycles)
62°C	30 sec	
95°C	15 sec	
62°C	30 sec	Melting Curve
95°C	30 sec	
60°C	15 sec	

3.7. Statistical analysis

Results are expressed as mean \pm standard deviation (SD) of at least 3 experiments in which the mRNA levels of vimentin are normalized to the mRNA levels of β -actin arbitrary set to 1, and of each 13 cells for fluorescence levels of caveolin, clathrin, CD44 receptor and P-glycoprotein. Student's t test was used for estimation of statistical significance (unpaired, two tails) for immunocytochemistry and mRNA expression results. Significance for statistical analysis was defined as $p < 0.05$.

4. Results

4.1. *In vitro* cytotoxicity of free salinomycin and loaded salinomycin

Monitoring cell viability and determination of the value of IC_{50}^1 in cell adherent culture is essential to compare the *in vitro* activity of free salinomycin (SAL) with that observed for the loaded salinomycin (PM_{sal}). The goal of analyzing the complexity of cell membrane response that emerges from the contact with exogenous samples in their proximity demands the determination of subtherapeutic concentrations for cell studies (*Table 4.1.I*). Thus, MDA-MB-231 cells were incubated with five different concentrations of plain micelles (PM)², loaded micelles and free salinomycin (PM_{sal} and SAL, respectively), for 24 and 48 hours.

After 24 hours of samples incubation, SAL promote a higher decrease in cell viability than PM_{sal} . The last one never promoting more than 50% of cell death in the concentration range tested. MDA-MB-231 cells incubated during 48 hours with SAL, exhibited a typical dose-dependent response, meaning that in the highest concentration the cell viability is almost non-existent (*Figure 4.1.I*). Either at 24 hours or 48 hours the “behavior” of PM and PM_{sal} was almost indistinguishable.

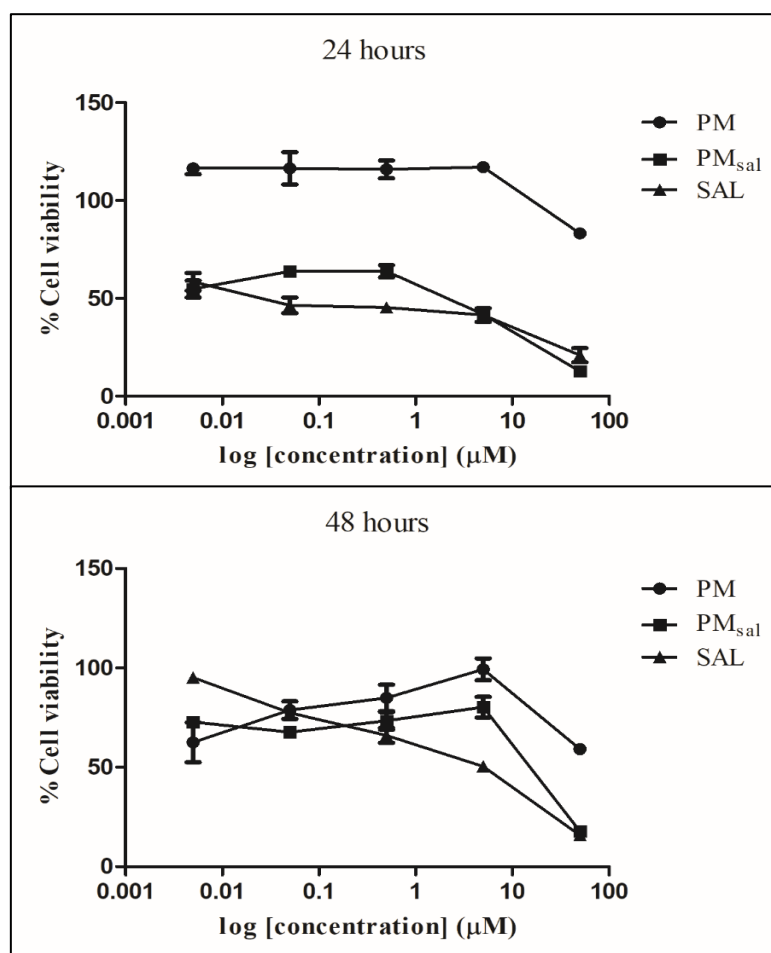


Figure 4.1.1 - MDA-MB-231 cell viability after 24 and 48 hours of incubation with plain micelles (PM), loaded micelles (PM_{sal}) and free salinomycin (SAL) in five different concentrations ([50 μM]; [5 μM]; [0.5 μM]; [0.05 μM]; [0.005 μM]).

¹ The IC_{50} is the concentration of an inhibitor where the response (or binding) is reduced by half. Sometimes it is confused with EC_{50} that designates the concentration of a drug that gives half-maximal response.

² For the five different concentrations of [50 μM]; [5 μM]; [0.5 μM]; [0.05 μM] and [0.005 μM], the polymer concentration used was [630 μg/ml]; [63 μg/ml]; [6.3 μg/ml]; [0.63 μg/ml] and [0.063 μg/ml], respectively.

The determined IC₅₀ value for PM_{sal} in MDA-MB-231 cells was 5.32 μ M and 51.94 μ M for 24 and 48 hours, respectively. For SAL the IC₅₀ value was 0.071 μ M at 24 hours and 5.34 μ M at 48 hours (*Table 4.1.1*).

Table 4.1.1 – IC₅₀ values (μ M) for free salinomycin (SAL) and loaded micelles (PM_{sal}) for 24 hours and 48 hours of incubation in MDA-MB-231 cells.

Incubation time	PM _{sal} (μ M)	SAL (μ M)
24 hours	5.32	0.071
48 hours	51.94	5.34

4.2. Nanoparticles functionalization with CD44v6 antibody

According to the manufacturer's instructions, for proteins with a molecular weight range from 20 to 150 kDa a 12% SDS-PAGE was made to assess the existence of free CD44v6 antibody on the functionalized plain micelles formulation (*Figure 4.2.1*). With CD44v6 antibody there were only two protein bands – one at 50 kDa and another at 25 kDa. For both functionalized and non-functionalized plain micelles (PM^{CD44} and PM, respectively) there was a blue smear below 35 kDa.

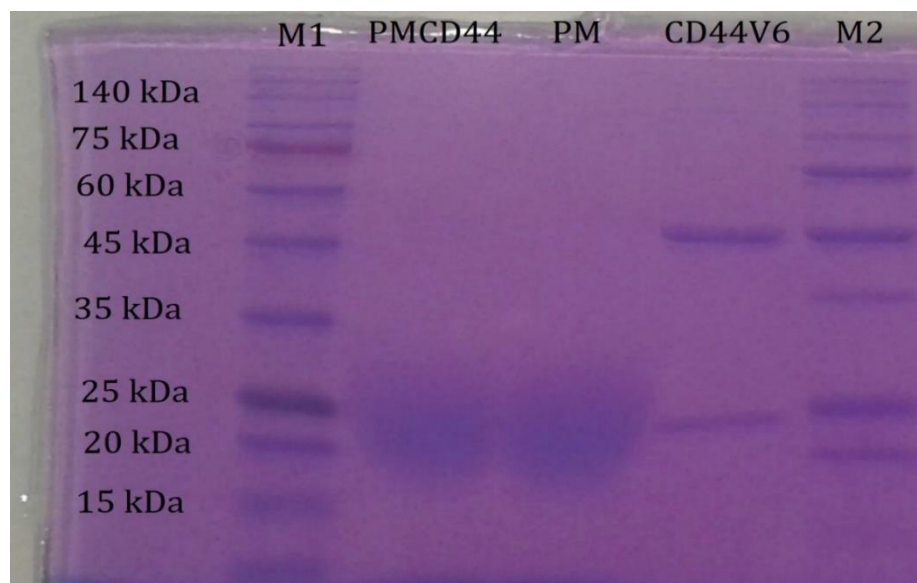


Figure 4.2.1 – 12% SDS-PAGE photography. This technique was used to evaluate the presence of free CD44v6 in the functionalized micelles dispersant phase. M1 – NZY colour protein marker I (molecular weight from 5 kDa to 245 kDa); PM^{CD44} – functionalized plain micelles with CD44v6 ([5 mg/ml/5 μ g/ml]); PM – plain micelles ([5 mg/ml]); CD44v6 – CD44v6 antibody used to functionalize the micelles ([5 μ g/ml]); M2 – Protein Marker (All blue prestained protein standards, BioRad) (molecular weight from 10k Da to 250 kDa)

4.3. Expression of endocytosis proteins after nanoparticle incubation

The experimental identification of membrane proteins involved in the NP uptake in MDA-MB-231 cells was set up by cells incubation with functionalized and non-functionalized plain micelles (PM^{CD44} and PM, respectively). Activity of caveolin and clathrin proteins as well as expression of CD44 receptor were evaluated.

In their basal state cells express high levels of CD44 receptor mainly in their membrane that translates to a fluorescence intensity of 24.9 a.u. Cell membrane contact with PM showed no changes on this receptor displayed fluorescence intensity, which means that CD44 receptor was not involved in PM internalization. This receptor recruitment response drastically changes in the presence of PM^{CD44} where the fluorescence intensity increased, approximately, two-folds, i.e., it changed from 25 to 47 a.u. (Figure 4.3.5).

In all the tested conditions, CD44 is highly expressed on cell membranes (Figure 4.3.1). Although not distinctly visible, cells incubated with PM exhibit small vesicles in the cytoplasm not visible on the PM^{CD44} cell experimental set. In the presence of PM^{CD44} CD44 receptors accumulate in certain domains that localize at the membrane surface (Figure 4.3.3).

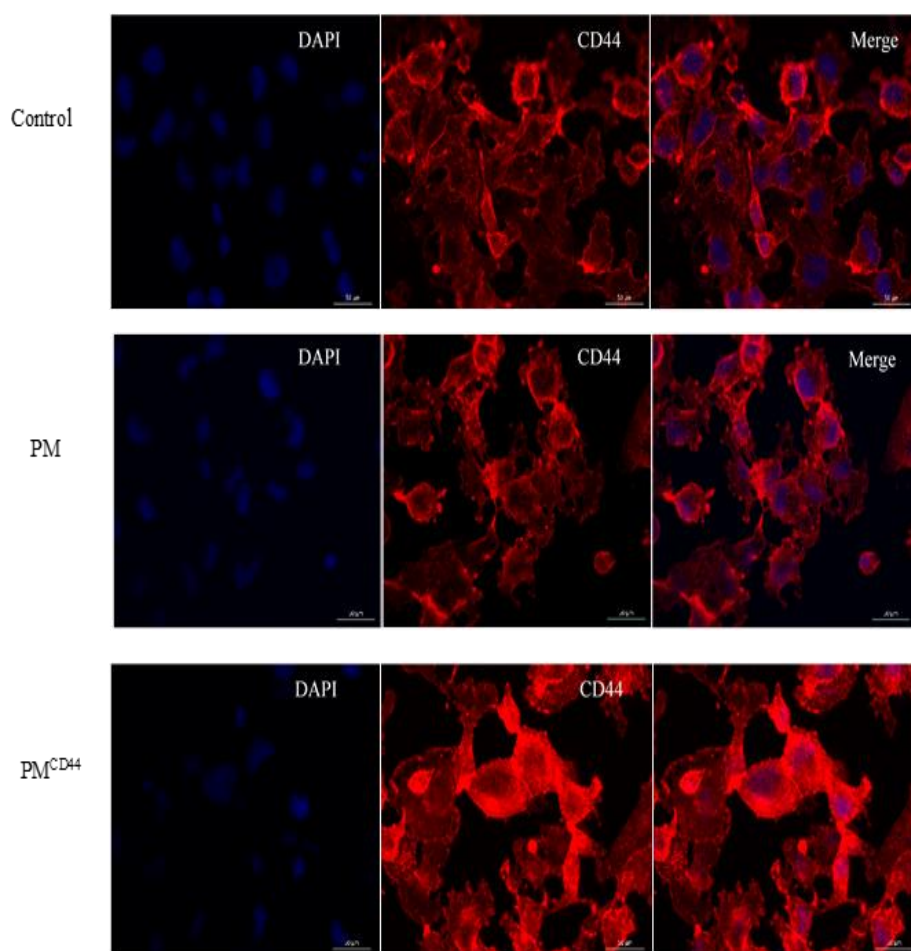


Figure 4.3.1 – Immunofluorescence of CD44 receptor in MDA-MB-231 cells in three different conditions after 30 minutes of incubation at 37°C: Control – cells were incubated with culture medium; PM – cells were incubated with [1 μM] of plain micelles; PM^{CD44} – cells were incubated with [1 μM] of functionalized plain micelles. Exposition time: 1500 ms. Scale bar: 50 μm .

When analyzing the cell membrane endocytic proteins behavior, we observed that the expression of clathrin did not differ from their basal state (control) upon MDA-MB-231 cells contact with PM and PM^{CD44} (Figure 4.3.2). The basal fluorescence intensity of clathrin was, approximately 20 a.u., which did not change in the presence of either PM or PM^{CD44} (Figure 4.3.5).

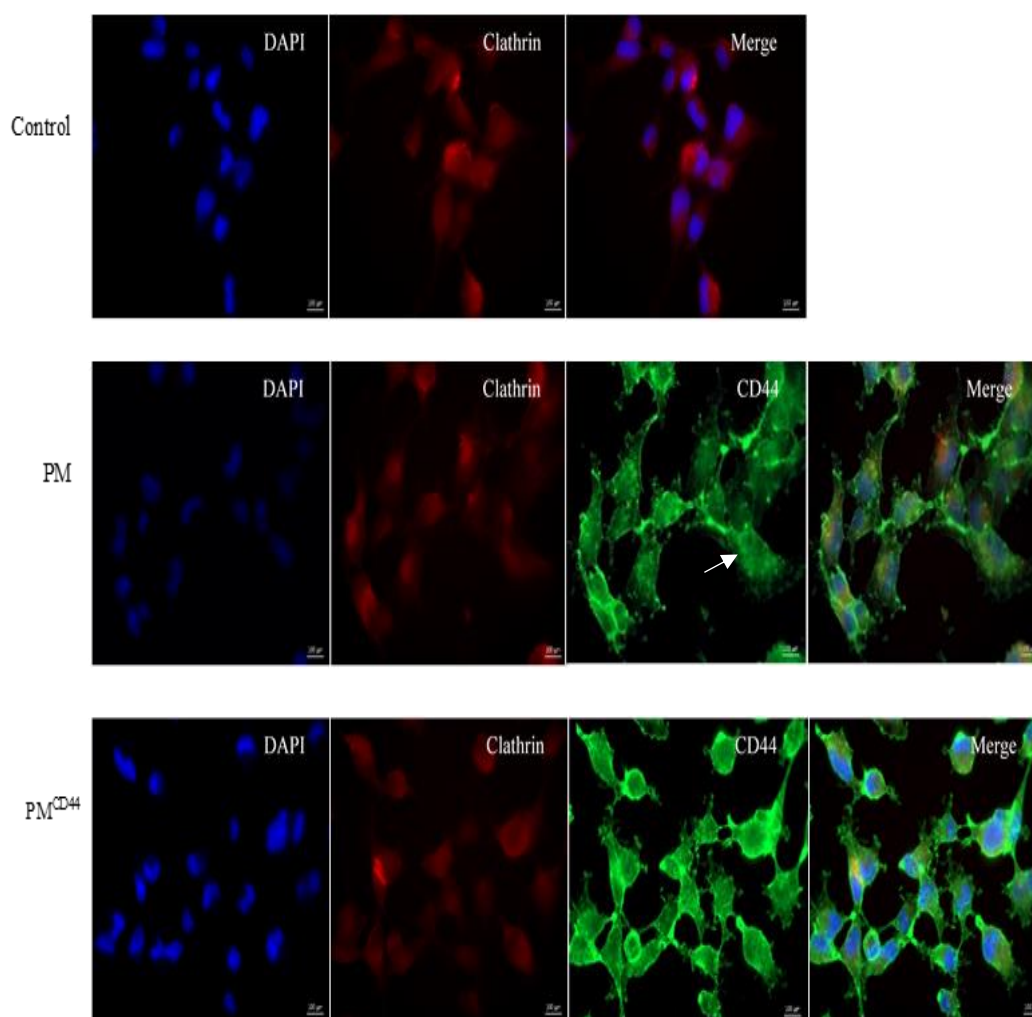


Figure 4.3.2 - Immunofluorescence of clathrin and CD44 receptor in MDA-MB-231 cells in three different conditions after 30 minutes of incubation at 37°C: Control – cells were incubated with culture medium; PM – cells were incubated with [1 μ M] of plain micelles; PM^{CD44} – cells were incubated with [1 μ M] of functionalized plain micelles. Exposition time: 4000 ms for clathrin and 1500 ms for CD44. Scale bar: 100 μ m.

On the contrary, membrane caveolin had a higher basal level of fluorescence intensity in MDA-MB-231 cell line. When incubated with PM the fluorescence intensity did not significantly change, but with PM^{CD44} there was an increase in the fluorescence intensity of caveolin (Figure 4.3.5). Cells incubated with PM clearly showed that caveolin proteins accumulated on the membrane surface in small domains. It was also visible the existence of small vesicles that contain CD44 but not caveolin. As expected, the presence of PM^{CD44} induced an increase in activity of caveolin and a recruitment of these proteins to form membrane domains in the same regions as CD44 (Figure 4.3.3 and Figure 4.3.4).

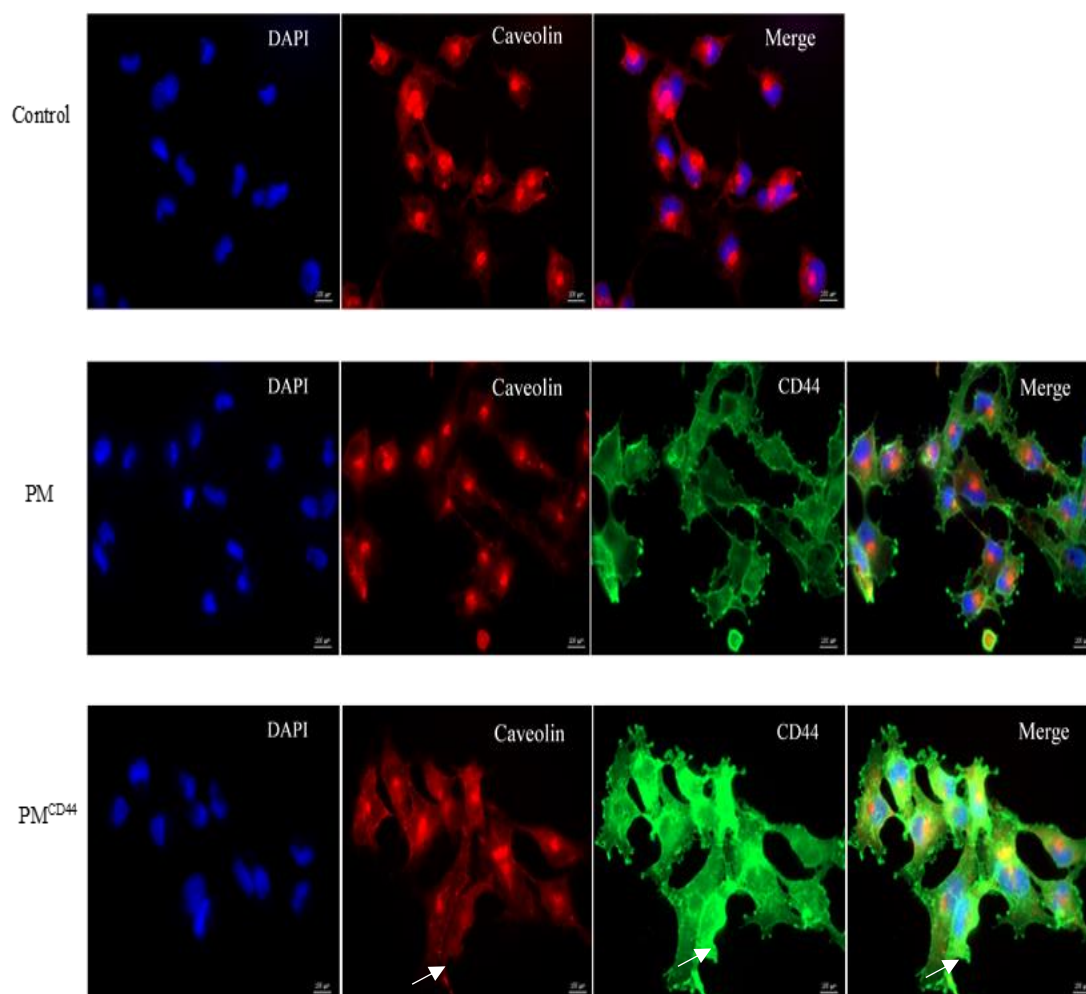


Figure 4.3.3 - Immunofluorescence of caveolin and CD44 receptor in MDA-MB-231 cells in three different conditions after 30 minutes of incubation at 37°C: Control – cells were incubated with culture medium; PM – cells were incubated with [1 μM] of plain micelles; PM^{CD44} – cells were incubated with [1 μM] of functionalized plain micelles. Exposition time: 5500 ms for caveolin and 1500 ms for CD44. Scale bar: 100 μm.

In a close up of the merge of the double staining of CD44 receptor and caveolin in the presence of PM^{CD44} (*Figure 4.3.3*), it is visible in some membrane domains a colocalization of caveolin proteins and CD44 receptor that, as stated above, has an increase in its fluorescence intensity (*Figure 4.3.4*).

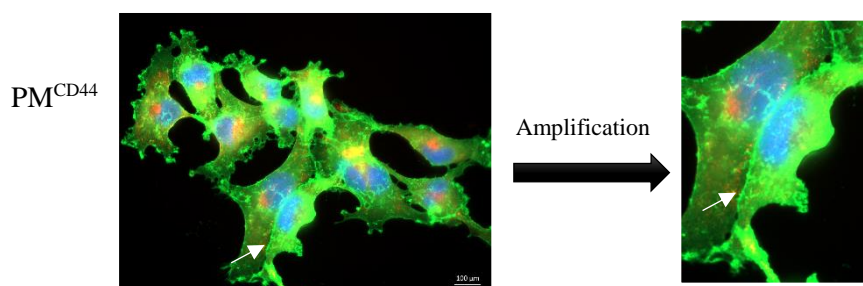


Figure 4.3.4 – Amplification of the merge from the double staining of CD44 receptor and caveolin proteins, where is evident a colocalization on certain membrane domains of CD44 receptor and caveolin proteins in MDA-MB-231 cells.

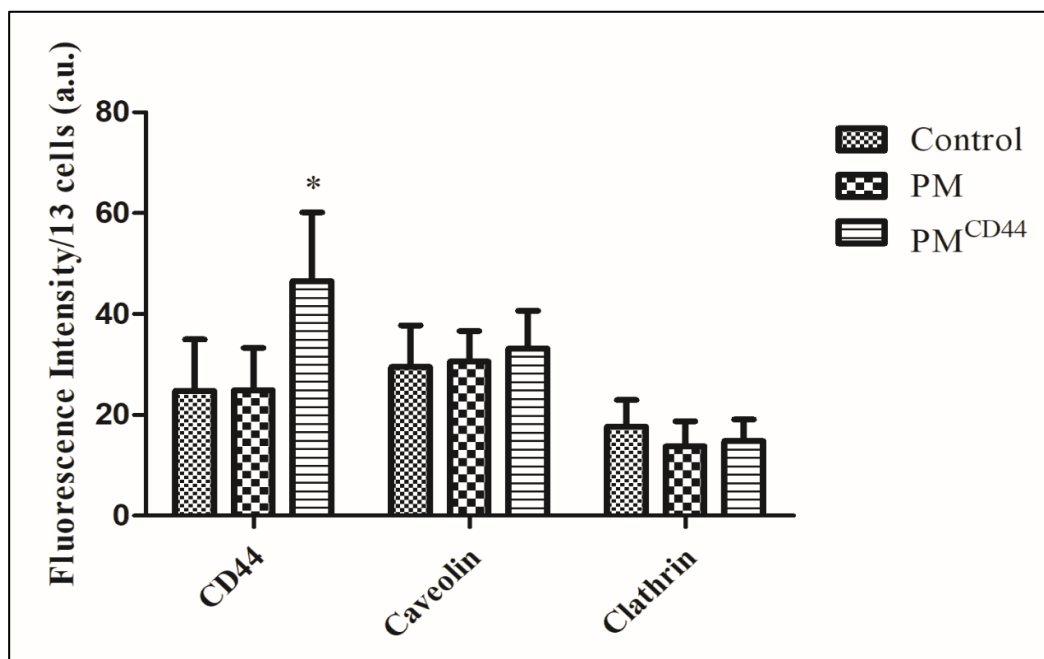


Figure 4.3.5 – Fluorescence intensity (a.u.) of CD44 receptor, caveolin and clathrin in three different conditions after 30 minutes of incubation: Control – cells were incubated with culture medium; PM – cells were incubated with [1 μ M] of plain micelles; PM^{CD44} – cells were incubated with [1 μ M] of functionalized plain micelles. Values represent the mean \pm SD for each 13 measurements. (* $p \leq 0.05$).

4.4. P-glycoprotein activity after incubation with loaded micelles and free salinomycin

To determine if the polymer used to make the NP would protect salinomycin from Pg-p's efflux, MDA-MB-231 cells were incubated with [1 μ M polymer] of PM, [1 μ M polymer/0.68 M_{sal}] of PM_{sal} and [0.68 μ M_{sal}] of SAL, for 30 minutes and 1 hour.

The fluorescence basal level of P-gp, after 30 minutes, was 15 a.u. which slightly increased with the presence of PM in the membrane vicinity. When incubated with PM_{sal} and SAL the fluorescence levels remained constant (*Figure 4.4.3*). Cells (control) where the P-gp was not stimulated shown this protein accumulation around the nucleus. This behavior changed when MDA-MB-231 cells were in contact with PM, with the observation that P-gp was no longer accumulated around the nucleus but in small vesicles in the cytoplasm. In the presence of PM_{sal} P-gp localized in vesicles in the cytoplasm (*Figure 4.4.1*).

More important and as expected owing the fact that SAL is a P-gp subtract, the presence of free drug increased this protein levels in the membrane (*Figure 4.1.1*).

After 1 hour, the basal fluorescence intensity of P-gp did not fluctuate when compared with the data from 30 minutes of incubation. At this point, there was a higher difference between the basal levels of P-gp and when in contact with SAL (*Figure 4.4.3*).

In all experiments, when not stimulated P-gp remained around the nucleus, and in contact with PM_{sal} there was an increased in the number of vesicles in the cytoplasm. Cells incubated with PM_{sal} and SAL, seemed to maintain the P-gp in the same cellular compartments as in the 30 minutes but with a higher fluorescence levels, especially with SAL (*Figure 4.4.2*).

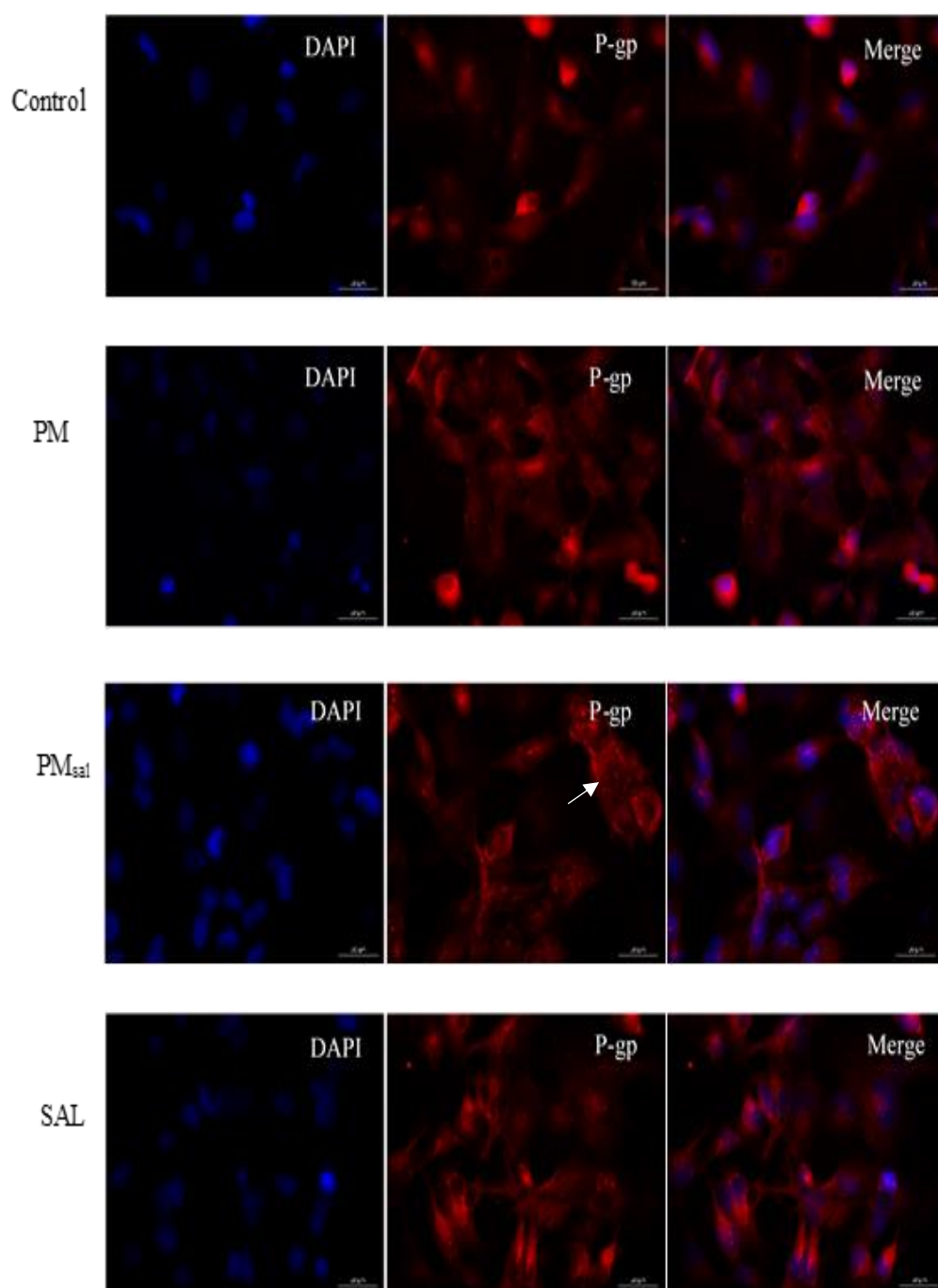


Figure 4.4.1 - Immunofluorescence of P-glycoprotein in MDA-MB-231 cells in three different conditions after 30 minutes of incubation at 37°C: Control – Cells were incubated with culture medium; PM – Cells were incubated with [1 µM polymer] of plain micelles; PM_{sal} – Cells were incubated with [1 µM polymer/0.68 µM sal] of loaded micelles; and SAL – Cells were incubated with [0.68 µM sal] of free salinomycin. Exposition time: 1500 ms. Scale bar: 50 µm

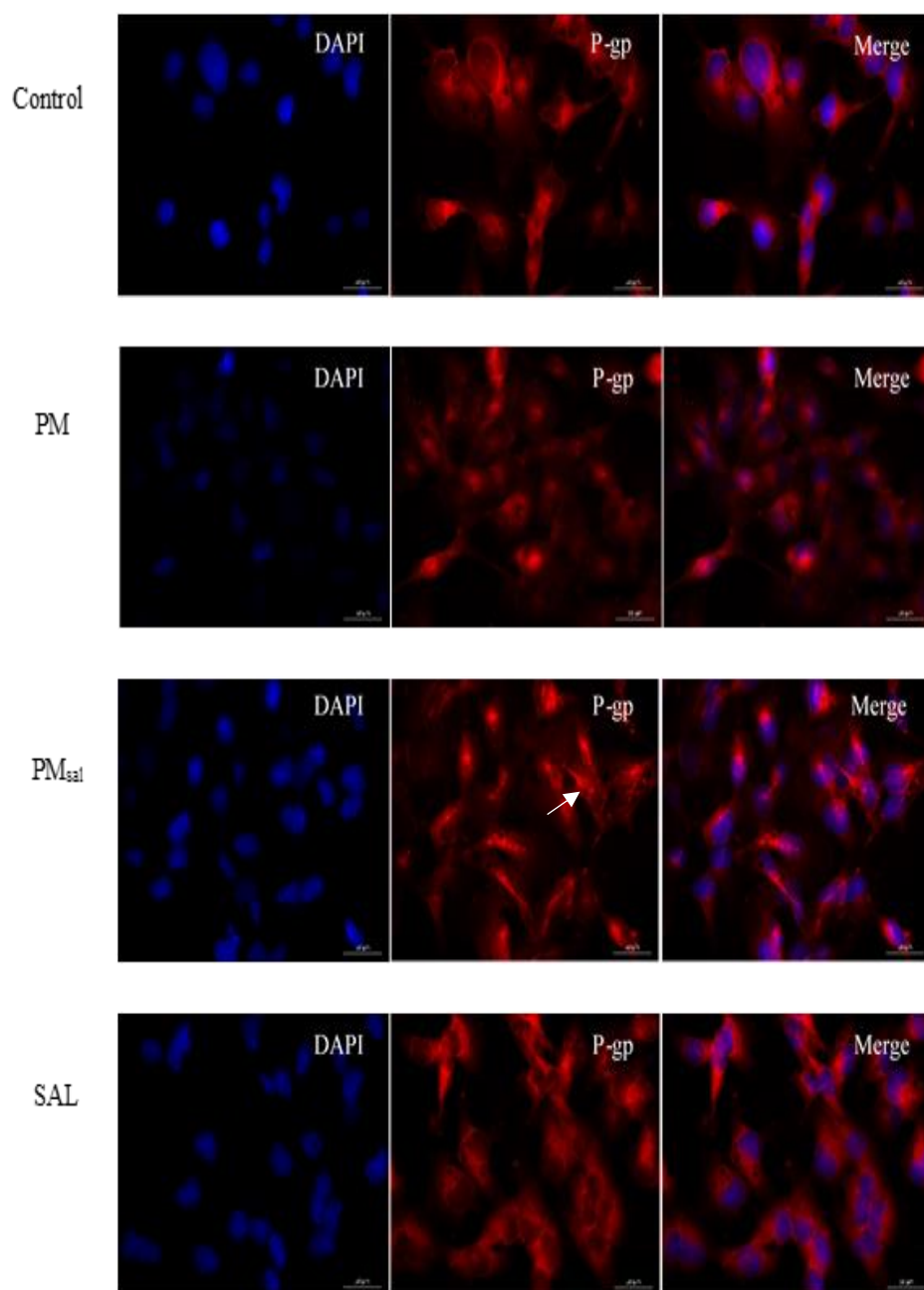


Figure 4.4.2 - Immunofluorescence of P-glycoprotein in MDA-MB-231 cells in three different conditions after 1 hour of incubation at 37°C: Control – Cells were incubated with culture medium; PM – Cells were incubated with [1 μ M polymer] of plain micelles; PM_{sal} – Cells were incubated with [1 μ M polymer/0.68 μ M sal] of loaded micelles; and SAL – Cells were incubated with [0.68 μ M sal] of free salinomycin. Exposition time: 1500 ms. Scale bar: 50 μ m

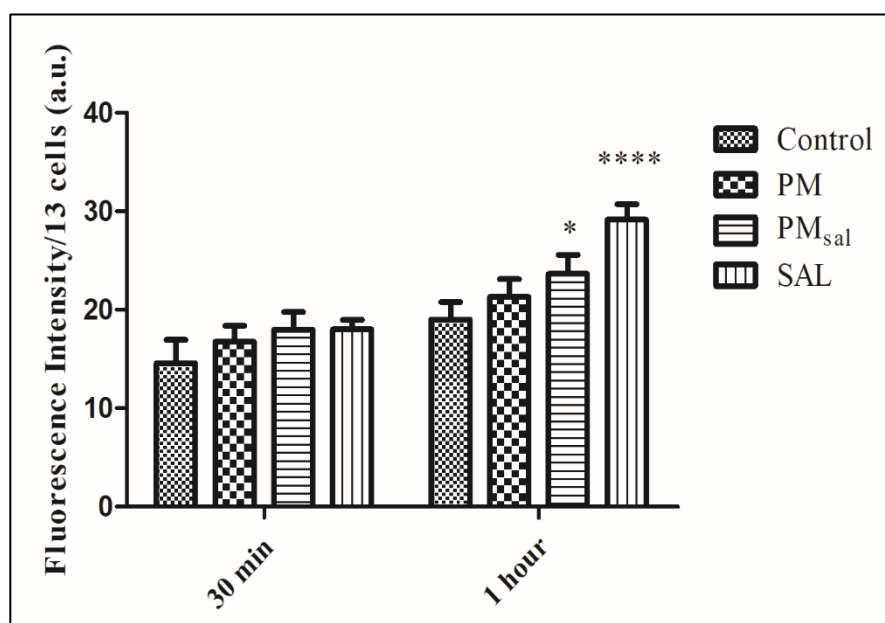


Figure 4.4.3 - Fluorescence intensity of P-glycoprotein in three different conditions after 30 minutes and 1 hour of incubation at 37°C: Control – Cells were incubated with culture medium; PM – Cells were incubated with [1 μ M polymer] of plain micelles; PM_{sal} – Cells were incubated with [1 μ M polymer/0.68 μ M_{sal}] of loaded micelles; and SAL – Cells were incubated with [0.68 μ M_{sal}] of free salinomycin. Values represent the mean \pm SD of each thirteen measurements. (* $p \leq 0.05$; **** $p \leq 0.0001$).

4.5. Vimentin expression modulation

The achievement of using PM_{sal}, as a therapeutically strategy against intracellular selective targets can be predicted by using a stemness protein cell level as a biomarker for malignancy. If attended, its translation inactivation decreases cell tumorigenesis thus affording cell death. To assess vimentin expression, using RT-qPCR, MDA-MB-231 cells were incubated with [0.05 M] and [1 μ M] of PM, PM_{sal} and SAL, for 48 and 72 hours.

After 48 hours of incubation cellular vimentin expression increased, approximately, 2-folds for [1 μ M] of PM_{sal} and SAL. When incubated with [0.05 M] of PM, PM_{sal} and SAL vimentin expression remained in its basal levels (control) (*Figure 4.5.1*).

72 hours afterwards, cells treated with [1 μ M] of PM_{sal} and SAL exhibited an increase in vimentin expression, approximately, 2-folds and 3-folds, respectively. As observed in the data from 48 hours, vimentin expression did not change when cells were incubated with [0.05 μ M] of PM, PM_{sal} and SAL (*Figure 4.5.1*).

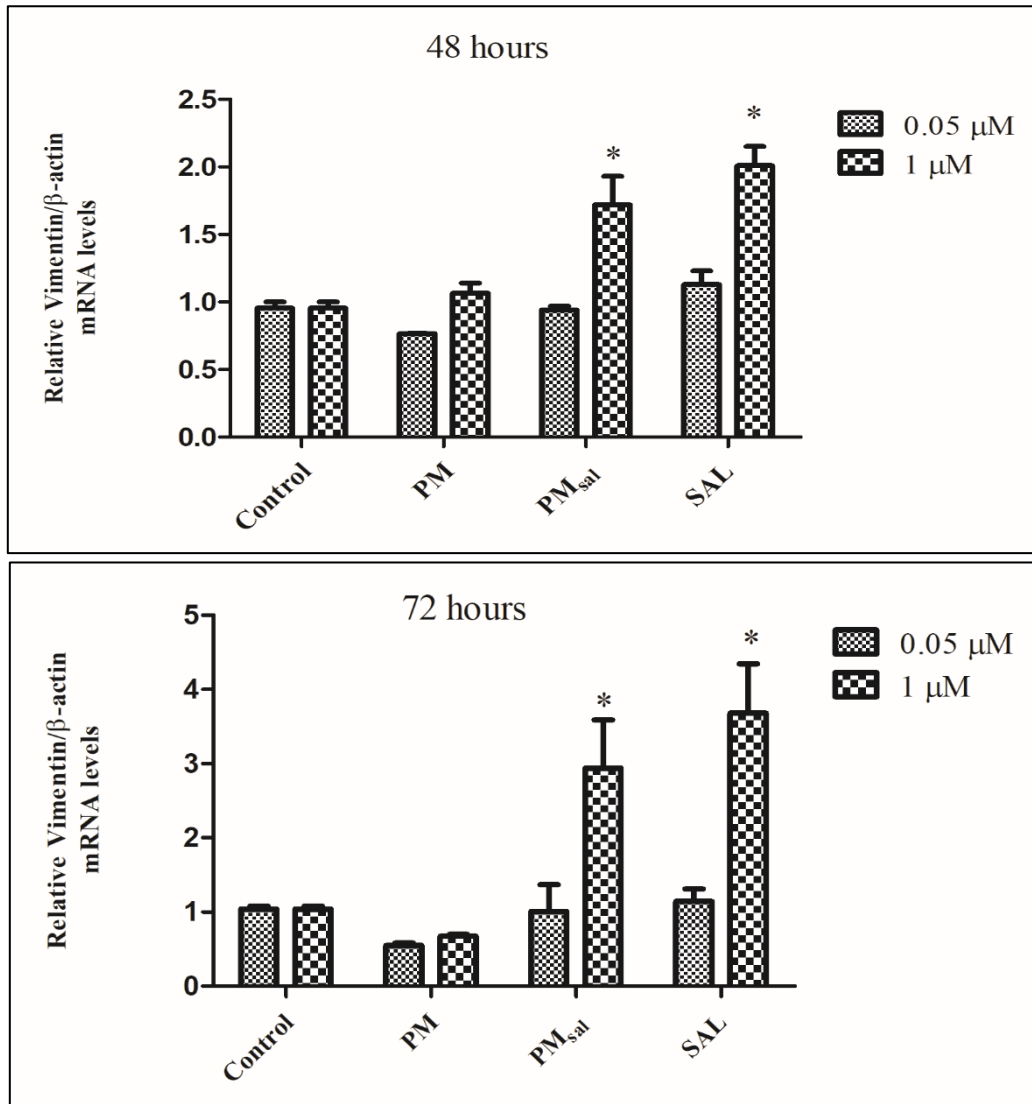


Figure 4.5.1 - RT-qPCR analysis performed in total mRNA isolated from MDA-MB-231 cells after 48 and 72 hours treatment with [0.05 μ M] and [1 μ M] of plain micelles (PM), loaded micelles (PM_{sal}) and free salinomycin (SAL). Relative vimentin mRNA levels are normalized to the expression of β -actin mRNA of each experiment. Values represent the mean \pm SD of each duplicate of the experiment. (* $p \leq 0.05$).

5. Discussion

The complexity of cell behavior's response to exogenous stimuli leads frequently to cell death. For this project it was necessary to establish both loaded and free drug, subtherapeutic doses of both formulation were used. With that purpose, determination of IC₅₀ was established for 24 hours and 48 hours (*Figure 4.1.1*). Whether at 24 hours or 48 hours the "behavior" of PM and PM_{sal} was almost identical, meaning the process by which they are uptaken is the same, indicating that there is no difference in the intracellular accumulation of salinomycin.

IC₅₀ dependency on incubation time and cell type⁴² explains the variation observed for salinomycin from 24 hours (0.071 μ M) to 48 hours (5.34 μ M). Those values, excluding the values from 24 hours, are in accordance with Ahmed *et al.* (2016), where the range values of IC₅₀ for salinomycin is between 0.3 and 10 μ M⁴². The apparent increase in cell viability might indicate an increase in cell number after 48 hours. This same result (data not shown) was exhibited in non-treated cells (control) where, after 48 hours of incubation, the number of cells duplicated.

According to Treuel *et al.* (2013), NP cell uptake can be influenced by their cycle phase. This study proves that upon 10 hours of incubation NP are divided between daughter cells⁵³. Since cancer cells have a higher proliferating rate than normal cells this effect is much more significant, and can thus influence the results observed in MTT assay, namely the variability observed in the extremes of the concentration range after 24 and 48 hours of incubation (*Figure 4.1.1*). It may also explain the increase in cell viability for SAL after 48 hours of incubation.

Importantly, high concentrations of PM_{sal} or PM promote alterations in cell morphology, namely a circular shape, with the consequently cell-detaching effect. It seems that after 24 hours, despite suspension cells that could be dead, we observed that these cells were able to adhere and recover its fibroblast-like morphology gaining also its proliferative ability. These fluctuations can explain inconsistencies in MTT data collect. Based on these data, the subtherapeutic concentrations chosen to study cell behavior were in the concentration range from [0.05 μ M] to [1 μ M].

In *Figure 4.1.1* (at 48 hours), a dose-dependent behavior and 100% cell viability for the lowest concentration can be observed. Cell death, displayed either by free or loaded salinomycin, is an indication that the drug is in fact downregulating cyclin D1⁴², and cells can no longer progress besides G1 phase, as described in the literature.

Unexpectedly, SAL when compared with PM_{sal} was more effective. Moreover, nanocarriers strategy to deliver drugs is based on their ability to increase drug intracellular accumulation⁴⁶. The similarity observed in cell viability upon incubation with plain and loaded micelles suggests PM_{sal} lack of drug release, which also justifies the higher pharmacological activity observed with the free drug. Wang *et al.* (2011) described that PTX-loaded micelles releasing rates can differ from 79% at pH 7.4 to 95% at pH 6.2. The authors observed that at low pH values the amino groups of the chitosan backbone are protonated, swelling the system and promoting drug release⁶². The same principle can be applied with PM_{sal}. For instance, since cancer cells are highly metabolic, the pH can decrease upon 48 hours of incubation which may influence the micelles structure thus releasing the drug in the extracellular space rather than in the intracellular compartments, diminishing the dose that is applied to the cancer cells.

Concerning the proteins involved in NP cell uptake or the CD44 receptor-mediated internalization, it was found that although MDA-MB-231 cells express clathrin proteins (*Figure 4.3.2*) the levels of fluorescence intensity do not change when cells are incubated with NP. Although clathrin basal levels did no change throughout the experiment, CD44 fluorescence level reached a maximum value when in the presence of PM^{CD44}. This allows us to conclude that clathrin is not involved in the NP uptake.

This was not expected since, according to Rejman *et al.* (2004), NP with a size below 200 nm would enter through clathrin-mediated endocytosis and only the ones with a size above 200 nm would

opt for a caveolae-mediated endocytosis⁵⁵. Taken into consideration that this work was performed with murine melanoma cells (B16-F10) and the present work uses human breast cancer cells, this result suggests that besides nanoparticle size, the type of cell used can influence the chosen endocytic pathway.

Though the levels of caveolin expression do not significantly change to the control both PM or PM^{CD44} an alteration in the activity of caveolin proteins can be detected (*Figure 4.3.3*) These results suggest a mediation by caveolae-mediated endocytosis NP have a similar behavior to the pathogens that also enter the cells through caveolae-mediated endocytosis to avoid lysosomal degradation⁵⁹.

Although clathrin-mediated endocytosis is the most common pathway for receptor-mediated endocytosis⁵⁴, in our study, the receptor-mediated players for functionalized nanocarrier (with PM^{CD44}) points to a caveolae-mediated endocytosis (*Figure 4.3.3*).

The fluorescence, corresponding to the CD44 membrane receptor, displayed by the non-incubated cells (control) is like the one that contact with the PM, suggesting that endocytosis of non-functionalized plain micelles do not involve the activity of CD44 (*Figure 4.3.1*). However, it is visible the existence of small vesicles in the cytoplasm of MDA-MB-231 CD44⁺ cells (*Figure 4.3.3*), suggesting the recruitment of this membrane receptor to the vesicle formation, even though the NP are not functionalized.

When cells were incubated with PM^{CD44}, CD44 membrane receptor expression double-folded (*Figure 4.3.5*) meaning that the connection of a nanoparticle functionalized with CD44v6 antibody increased the number of receptors at the membrane. Since free CD44v6 antibody can saturate the membrane surface receptors and prevent the interaction of PM^{CD44} with CD44 membrane surface receptor, it is important to ensure that no free CD44V6 antibody exists in the formulation (PM^{CD44}).

That being said, results from protein quantification (*Figure 4.2.1*) showed that free CD44v6 antibody presents only two protein bands – one at 50 kDa that corresponds to the heavy chain and another at 25 kDa that represents the light chain. These same protein bands do not appear within the functionalized micelles meaning that there is no free antibody in the formulation (PM^{CD44}). These data plus the results obtained with the endocytosis assay, where the fluorescence intensity of CD44 increased with PM^{CD44}, allows us to conclude that the amount of antibody used to functionalize the micelles was attached to their surface. However, we could not determine if the concentration of CD44v6 used ([5 µg/ml]) is enough to saturate all the cell membrane surface receptors.

The results appear to suggest that interaction of CD44v6 antibody with the membrane receptor resulted in the activation of CD44, and probably, to its proteolytic cleavage and the resulting intracellular fragment translocated to the nucleus and activated transcription of CD44 gene^{26,29}. Evidently this would have to be confirmed by mRNA analysis, to assess the increased expression of CD44.

Along with the increase of CD44 expression, it is important to note that when cells are in contact with PM^{CD44} they respond with a caveolin accumulation in certain domains of the membrane, that coincidentally were the same were CD44 was also present (*Figure 4.3.4*). These domains could potentially be lipid rafts (more specifically caveolae), although we would have to stain other components present in lipid rafts (such as ceramides) to be sure that those are in fact lipid rafts, but apparently the results point to that way since CD44 localizes in lipid rafts³² and the main component of caveolae (a form of specialized lipid rafts) is caveolin⁶⁰. These data appear to be in accordance with the results of Qhattal *et al.* (2011), where CD44-mediated internalization of HA-liposomes occurs via lipid rafts⁶³.

Differences observed in the internalization rate between PM^{CD44} and PM highlighted the CD44 membrane receptor recruitment. These data are in agreement with previous studies, where endocytosis of functionalized NP is delayed in the first 30 minutes and its maximum is at 4 hours of incubation^{64,65}.

As for the P-gp involvement, it is important to recognize that P-gp can be localized in many cellular organelles, such as endoplasmic reticulum, Golgi and endosomal compartments⁶⁶. When not stimulated P-gp remains mostly around the nucleus (*Figure 4.4.1* and *Figure 4.4.2*), which will correspond to the endoplasmic reticulum and perhaps to Golgi apparatus, although counter staining with markers for each one of the cellular components is required. Data are in accordance with other

investigations, where there was no localization of P-gp in the nucleus⁶⁷. Although the fluorescence level of P-gp slightly increases from 30 min to 1 hour (*Figure 4.4.3*), the cellular localization of this protein does not change.

After incubation with PM (30 minutes and 1 hour) (*Figure 4.4.3*), the level of fluorescence does not change when compared to the control. This could mean that the polymer does not stimulate P-gp activity. In the presence of PM_{sal}, cells no longer appear to have a high concentration of P-gp around the nucleus, because it is dispersed all around the cytoplasm, in small vesicles (*Figure 4.4.1*) that will increase in number upon 1 hour of incubation (*Figure 4.4.2*). Vesicles closer to the cell membrane would correspond to early endosomes or recycling endosomes, since P-gp can be localized in both⁶⁷. These data indicate that micelles can be recycled up at least to 1 hour. Stressing out the data from MTT assay, we propose that micelles are recycled until 24 hours after incubation. It would be interesting to see the localization of P-gp throughout this time, with other components of the endocytic pathway, such as Rab GTPases.

Cell response to the free drug was denoted with the increase of P-gp fluorescence corresponding to the staining of P-gp. This behavior has its maximum upon 1 hour of incubation with the fluorescence increasing compared to the control (*Figure 4.4.3*). Even though the fluorescence level 30 minutes after incubation does not change for all tested samples (PM, PM_{sal} and SAL), cells incubated with free salinomycin display a slightly P-gp accumulation predominantly in endoplasmic reticulum, and Golgi apparatus, although it still exists a high quantity of this protein in the membrane surface (*Figure 4.4.1*). P-gp accumulation in the endoplasmic reticulum, Golgi apparatus, and plasma membrane increases upon 1 hour (*Figure 4.4.2*), which could indicate an increase in P-gp expression in these cellular compartments due to salinomycin intracellular accumulation⁶⁷.

Even though cells display a slightly different pattern (1 hour) when comparing P-gp expression when treated with SAL against those treated with PM_{sal}, it is our conviction that these events might have a crucial importance (*Figure 4.4.2*). The data suggest that P-gp predominantly localizes in endoplasmic reticulum and, perhaps Golgi, and in the plasma membrane, which means that P-gp is reacting to intracellular salinomycin (*Figure 4.4.1* and *Figure 4.4.2*). According to Fu *et al.* (2004), a high level of drug resistance happens when P-gp accumulates in endoplasmic reticulum and Golgi, and in the membrane surface, although in less quantity in this last one – as a result of drug accumulation⁶⁷. This means that whether it is 30 minutes or 1 hour, salinomycin is released from micelles in a cellular organelle that has a pH between 7.4-6.2, in order to protonate the amino groups of the polymer⁶², as stated above. This organelle could possibly be recycling endosomes or early endosomes. There is also some vesicles in the cytoplasm with P-gp, which means that although most of P-gp is used to respond to the drug in the cytoplasm a small quantity is recycled back to the membrane⁶⁶.

Vimentin cell expression was used to clarify PM_{sal} efficacy and compared with that of free drug. Although unexpected, loaded micelles and free salinomycin increased the expression of EMT marker vimentin by more than two-folds (*Figure 4.5.1*). These data are in accordance with the results obtained by Kuo *et al.* (2012), where there was an increased in vimentin expression with salinomycin treatment, at the same time Akt phosphorylation increased⁶⁸. This is not surprising since Zhu *et al.* (2011), demonstrated that inhibition of AKT1 leads to proteolysis of vimentin, and eventually cell death, and that phosphorylation of vimentin by AKT1 blocked caspase-induced apoptosis²¹. These data allow us to conclude that salinomycin may phosphorylate Akt, leading to vimentin phosphorylation, blocking caspase-induced apoptosis.

These results suggest that loaded salinomycin may not be the best stand-alone therapy for killing breast cancer stem cells since the value of IC50 for encapsulated salinomycin is higher, approximately 5 to 10 folds for 24 and 48 hours, respectively, than free salinomycin. This translates into a higher dose of the drug to have the same effect in 50% of breast cancer cells.

It can also be hypothesized, based on the data from *Figure 4.1.1*, that in the first 24 hours micelles (PM and PM_{sal}) are being recycled back to the exterior. From the endocytosis assay, these micelles are uptaken through caveolae-mediated endocytosis to avoid lysosomal degradation. If, in fact, micelles did reach lysosomal compartments, they would be degraded and enhance cell toxicity⁶⁹, leading to a decrease in cell viability that is only visible after 48 hours of incubation. Besides this, there is a concentration range where cell viability is constant, which means that neither PM or PM_{sal} are affecting the molecular pathways.

6. Conclusion

From this work one thing is clear. There is so much that is still unknown when it comes to the way cancer cells modify their cellular mechanisms when compared to normal cells. For the first 24 hours it is possible that micelles are being recycled in and out of the cell and that salinomycin is being freed outside the cells.

When using micelles to deliver cytotoxic drugs to breast cancer stem cells, the uptake is made through caveolae-dependent endocytosis that does avoid lysosomal degradation. Functionalized micelles are uptaken through a CD44-dependent endocytosis, that has the intervention of caveolin proteins and results in the increase of CD44 expression at membrane surface, and their entry is delayed at least 30 minutes.

The fact that localization of P-gp does not change from non-treated cells to cells treated only with plain micelles means that these micelles do not create any type of resistance, so it is a good indicator that future therapies with this transporter are a safe bet. However, after 1 hour of incubation with loaded salinomycin, P-gp still localizes in the same places when incubated with free salinomycin, but it happens in a smaller scale.

It was clear that salinomycin may not be the best stand-alone therapy, due its apparent ability to enhance the metastatic potential of the cells by upregulating vimentin expression, but it could be a good therapeutic drug to inhibit P-gp activity copulated with other treatments.

7. References

1. Johns Hopkins Medicine. Breast Cancer and Breast Pathology. Available at: <http://pathology.jhu.edu/breast/index.php>. (Accessed: 17th June 2017)
2. Videira, M., Reis, R. L. & Brito, M. A. Deconstructing breast cancer cell biology and the mechanisms of multidrug resistance. *Biochim. Biophys. Acta* 1846, 312–325 (2014).
3. McDermott, S. P. & Wicha, M. S. Targeting breast cancer stem cells. *Mol. Oncol.* 4, 404–419 (2010).
4. Stockmans, G., Deraedt, K., Wildiers, H., Moerman, P. & Paridaens, R. Triple-negative breast cancer. *Curr. Opin. Obstet. Gynecol.* 20, 614–620 (2015).
5. Bartsch, R., Ziehermayr, R., Zielinski, C. C. & Steger, G. G. Triple-negative breast cancer. *Wiener Medizinische Wochenschrift* 160, 174–181 (2010).
6. Dawood, S. Triple-Negative Breast Cancer - Epidemiology and Management Options. *Drugs* 70, 2247–2258 (2010).
7. Ahn, S. G., Kim, S. J., Kim, C. & Jeong, J. Molecular classification of triple-negative breast cancer. *J. Breast Cancer* 19, 223–230 (2016).
8. Lehmann, B. D. *et al.* Identification of human triple-negative breast cancer subtypes and preclinical models for selection of targeted therapies. *J. Clin. Invest.* 121, 2750–2767 (2011).
9. Angeloni, V., Tiberio, P., Appierto, V. & Daidone, M. G. Implications of stemness-related signaling pathways in breast cancer response to therapy. *Semin. Cancer Biol.* 1–9 (2014).
10. Clarke, M. F. *et al.* Cancer stem cells - Perspectives on current status and future directions: AACR workshop on cancer stem cells. *Cancer Res.* 66, 9339–9344 (2006).
11. Dewangan, J., Srivastava, S. & Rath, S. K. Salinomycin: A new paradigm in cancer therapy. *Tumor Biol.* 39, 101042831769503 (2017).
12. Naujokat, C. & Steinhart, R. Salinomycin as a drug for targeting human cancer stem cells. *J. Biomed. Biotechnol.* 2012, 44–46 (2012).
13. Foulkes, W. D., Smith, I. E. & Reis-Filho, J. S. Triple-Negative Breast Cancer. *N. Engl. J. Med.* 20, 1938–1948 (2010).
14. Chacón, R. D. & Costanzo, M. V. Triple-negative breast cancer. *Breast Cancer Res.* 12, 1–9 (2010).
15. Yan, Y., Zuo, X. & Wei, D. Emerging Role of CD44 in Cancer Stem Cells: A Promising Biomarker and Therapeutic Target. *Stem Cells Transl. Med.* 4, 1033–43 (2015).
16. Lamouille, S., Xu, J. & Derynck, R. Molecular mechanisms of epithelial-mesenchymal transition. *Natl. Rev. Mol. Cell Biol.* 15, 178–196 (2014).
17. Kidd, M. E., Shumaker, D. K. & Ridge, K. M. The role of Vimentin intermediate filaments in the progression of lung cancer. *Am. J. Respir. Cell Mol. Biol.* 50, 1–6 (2014).
18. Cogli, L., Progida, C., Bramato, R. & Bucci, C. Vimentin phosphorylation and assembly are regulated by the small GTPase Rab7a. *Biochim. Biophys. Acta - Mol. Cell Res.* 1833, 1283–1293 (2013).
19. Barberis, L. *et al.* Leukocyte transmigration is modulated by chemokine-mediated PI3K γ -dependent phosphorylation of vimentin. *Eur. J. Immunol.* 39, 1136–1146 (2009).
20. Satelli, A. & Li, S. Vimentin in cancer and its potential as a molecular target for cancer therapy. *Cell. Mol. Life Sci.* 68, 3033–3046 (2011).

21. Zhu, Q.-S. *et al.* Vimentin is a novel AKT1 target mediating motility and invasion. *Oncogene* 30, 457–470 (2011).
22. Alonso-Curbelo, D. *et al.* RAB7 Controls Melanoma Progression by Exploiting a Lineage-Specific Wiring of the Endolysosomal Pathway. *Cancer Cell* 26, 61–76 (2014).
23. Margiotta, A., Progida, C., Bakke, O. & Bucci, C. Rab7a regulates cell migration through Rac1 and vimentin. *Biochim. Biophys. Acta - Mol. Cell Res.* 1864, 367–381 (2016).
24. Louderbough, J. M. V. & Schroeder, J. A. Understanding the Dual Nature of CD44 in Breast Cancer Progression. *Mol. Cancer Res.* 9, 1573–1586 (2011).
25. Cichy, J. & Puré, E. The liberation of CD44. *J. Cell Biol.* 161, 839–843 (2003).
26. Thorne, R. F., Legg, J. W. & Isacke, C. M. The role of the CD44 transmembrane and cytoplasmic domains in co-ordinating adhesive and signalling events. *J. Cell Sci.* 117, 373–380 (2003).
27. Morath, I., Hartmann, T. N. & Orian-Rousseau, V. CD44: More than a mere stem cell marker. *Int. J. Biochem. Cell Biol.* 81, 166–173 (2016).
28. Hahn, S., Gehri, R. & Erb, P. Mechanism and biological significance of CD44 cleavage. *Cancer Science* 95, 930–935 (1995).
29. Heldin, P. *et al.* Importance of hyaluronan-CD44 interactions in Inflammation and Tumorigenesis. *Connect. Tissue Res.* 49, 215–8 (2008).
30. Thomas, L., Etoh, T., Stamenkovic, I., Mihm, M. C. & Byers, H. R. Migration of Human Melanoma Cells on Hyaluronate Is Related to CD44 Expression. *J. Invest. Dermatol.* 100, 115–120 (1993).
31. Su, Y.-J., Lai, H.-M., Chang, Y.-W., Chen, G.-Y. & Lee, J.-L. Direct reprogramming of stem cell properties in colon cancer cells by CD44. *EMBO J.* 30, 3186–3199 (2011).
32. Babina, I. S., McSherry, E. a, Donatello, S., Hill, A. D. & Hopkins, A. M. A novel mechanism of regulating breast cancer cell migration via palmitoylation-dependent alterations in the lipid raft affiliation of CD44. *Breast Cancer Res.* 16, 1–14 (2014).
33. Horta, S. *et al.* Looking out for Cancer Stem Cells' Properties: The Value-Driving Role of CD44 for Personalized Medicines. *Curr. Cancer Drug Targets* 14, 832–849 (2015).
34. Negi, L. M. *et al.* Role of CD44 in tumour progression and strategies for targeting. *J. Drug Target.* 20, 561–573 (2012).
35. Brown, R. L., Reinke, L. M., Damerow, M. S. & Perez, D. CD44 splice isoform switching in human and mouse epithelium is essential for epithelial-mesenchymal transition and breast cancer progression. *J. Clin. Invest.* 121, 1064–1074 (2011).
36. Mielgo, A., van Driel, M., Bloem, A., Landmann, L. & Günthert, U. A novel antiapoptotic mechanism based on interference of Fas signaling by CD44 variant isoforms. *Cell Death Differ.* 13, 465–477 (2006).
37. Maldonado-Báez, L., Cole, N. B., Krämer, H. & Donaldson, J. G. Microtubule-dependent endosomal sorting of clathrin-independent cargo by Hook1. *J. Cell Biol.* 201, 233–247 (2013).
38. Lopez, J. I. *et al.* CD44 Attenuates Metastatic Invasion during Breast Cancer Progression. *Cancer Res.* 65, 6755–6764 (2005).
39. Sui, H., Fan, Z. Z. & Li, Q. Signal transduction pathways and transcriptional mechanisms of ABCB1/Pgp-mediated multiple drug resistance in human cancer cells. *J Int Med Res* 40, 426–435 (2012).
40. Amin, L. P-glycoprotein Inhibition for Optimal Drug Delivery. *Drug Target Insights* 7, 27–34

- (2013).
41. Katayama, K., Noguchi, K. & Sugimoto, Y. Regulations of P-Glycoprotein/ABCB1/MDR1 in Human Cancer Cells. *New J. Sci.* 2014, 1–11 (2014).
 42. Ahmed, K., Shaw, H. V., Koval, A. & Katanaev, V. L. A second WNT for old drugs: Drug repositioning against WNT-dependent cancers. *Cancers (Basel)*. 8, 1–27 (2016).
 43. An, H. *et al.* Salinomycin possesses anti-tumor activity and inhibits breast cancer stem-like cells via an apoptosis-independent pathway. *Biochem. Biophys. Res. Commun.* 466, 696–703 (2015).
 44. Bourguignon, L. Y. W., Peyrollier, K., Xia, W. & Gilad, E. Hyaluronan-CD44 Interaction Activates Stem Cell Marker Nanog, Stat-3-mediated MDR1 Gene Expression, and Ankyrin-regulated Multidrug Efflux in Breast and Ovarian Tumor Cells. *J. Biol. Chem.* 283, 17635–17651 (2008).
 45. Miletti-González, K. E. *et al.* The CD44 Receptor Interacts with P-glycoprotein to Promote Cell Migration and Invasion in Cancer. *Cancer Res.* 65, 6660–6667 (2005).
 46. Torchilin, V. P. Targeted polymeric micelles for delivery of poorly soluble drugs. *Cell. Mol. Life Sci.* 61, 2549–2559 (2004).
 47. Kumari, A., Yadav, S. K. & Yadav, S. C. Biodegradable polymeric nanoparticles based drug delivery systems. *Colloids Surfaces B Biointerfaces* 75, 1–18 (2010).
 48. Duncan, R. Polymer conjugates as anticancer nanomedicines. *Nat. Rev. Cancer* 6, 688–701 (2006).
 49. Plattt, V. M. & Szoka, F. C. Anticancer Therapeutics: Targeting Macromolecules and Nanocarriers to Hyaluronan or CD44, a Hyaluronan Receptor. *Mol. Pharm.* 5, 474–486 (2008).
 50. Danhier, F., Feron, O. & Préat, V. To exploit the tumor microenvironment: Passive and active tumor targeting of nanocarriers for anti-cancer drug delivery. *J. Control. Release* 148, 135–146 (2010).
 51. Bahrami, B. *et al.* Nanoparticles and targeted drug delivery in cancer therapy. *Immunol. Lett.* 190, 64–83 (2017).
 52. Champion, J. A., Walker, A. & Mitragotri, S. Role of particle size in phagocytosis of polymeric microspheres. *Pharm. Res.* 25, 1815–21 (2008).
 53. Treuel, L., Jiang, X. & Nienhaus, G. U. New views on cellular uptake and trafficking of manufactured nanoparticles. *J. R. Soc. Interface* 10, 20120939 (2013).
 54. Oh, N. & Park, J. H. Endocytosis and exocytosis of nanoparticles in mammalian cells. *Int. J. Nanomedicine* 9, 51–63 (2014).
 55. Rejman, J., Oberle, V., Zuhorn, I. S. & Hoekstra, D. Size-dependent internalization of particles via the pathways of clathrin- and caveolae-mediated endocytosis. *Biochem. J.* 377, 159–69 (2004).
 56. Kuhn, D. A. *et al.* Different endocytotic uptake mechanisms for nanoparticles in epithelial cells and macrophages. *Beilstein J. Nanotechnol.* 5, 1625–1636 (2014).
 57. Sahay, G., Alakhova, D. Y. & Kabanov, A. V. Endocytosis of Nanomedicine. *J. Control. Release* 145, 182–195 (2010).
 58. Kou, L., Sun, J., Zhai, Y. & He, Z. The endocytosis and intracellular fate of nanomedicines: Implication for rational design. *Asian J. Pharm. Sci.* 8, 1–8 (2013).
 59. Medina-Kauwe, L. K. ‘Alternative’ Endocytic Mechanisms Exploited by Pathogens. *Adv. Drug Deliv. Rev.* 70, 646–656 (2013).

60. Ramsay, A. G., Marshall, J. F. & Hart, I. R. Integrin trafficking and its role in cancer metastasis. *Cancer Metastasis Rev.* 26, 567–578 (2007).
61. Lajoie, P. & Nabi, I. R. *Lipid rafts, caveolae, and their endocytosis. International Review of Cell and Molecular Biology* 282, (Elsevier Inc., 2010).
62. Wang, F. *et al.* Folate-mediated targeted and intracellular delivery of paclitaxel using a novel deoxycholic acid-O-carboxymethylated chitosan-folic acid micelles. *Biomaterials* 32, 9444–9456 (2011).
63. Qhattal, H. S. S. & Liu, X. Characterization of CD44-Mediated Cancer Cell Uptake and Intracellular Distribution of Hyaluronan-Grafted Liposomes. *Mol. Pharm.* 70, 646–656 (2011).
64. Gao, H. *et al.* Ligand modified nanoparticles increases cell uptake, alters endocytosis and elevates glioma distribution and internalization. *Sci. Rep.* 3, 2534 (2013).
65. Cavaco, M. C. *et al.* Evading P-glycoprotein mediated-efflux chemoresistance using Solid Lipid Nanoparticles. *Eur. J. Pharm. Biopharm.* 110, 76–84 (2017).
66. Fu, D., Nobili, S. & William Murray, B. Where is it and how does it get there – intracellular localization and traffic of P-glycoprotein. *Front. Oncol.* 3, 1–5 (2013).
67. Fu, D., Bebawy, M., Kable, E. P. W. & Roufogalis, B. D. Dynamic and intracellular trafficking of P-glycoprotein-EGFP fusion protein: Implications in multidrug resistance in cancer. *Int. J. Cancer* 109, 174–181 (2004).
68. Kuo, S. Z. *et al.* Salinomycin induces cell death and differentiation in head and neck squamous cell carcinoma stem cells despite activation of epithelial-mesenchymal transition and Akt. *BMC Cancer* 12, 556 (2012).
69. Saptarshi, S. R., Duschl, A. & Lopata, A. L. Interaction of nanoparticles with proteins: relation to bio-reactivity of the nanoparticle. *J. Nanobiotechnology* 11, 26 (2013).